Moxifloxacin-mediated killing of *Mycobacterium tuberculosis* involves respiratory downshift, reductive stress, and ROS accumulation

Somnath Shee[1, 2 ¶], Samsher Singh[1, 2 ¶], Ashutosh Tripathi[1, 2], Chandrani Thakur[3], Anand Kumar T[4], Mayashree Das[1, 2], Vikas Yadav[1, 2], Sakshi Kohli[1, 2], Raju S. Rajmani[2], Nagasuma Chandra[3], Harinath Chakrapani[4], Karl Drlica[5 *], Amit Singh[1, 2 *]

[1]Department of Microbiology and Cell Biology, [2]Centre for Infectious Disease Research, Indian Institute of Science, Bangalore 560012, Karnataka, India

[3]Department of Biochemistry, Indian Institute of Science, Bangalore 560012, Karnataka, India

[4]Department of Chemistry, Indian Institute of Science Education and Research (IISER) Pune, Pune 411 008, Maharashtra, India

[5]Public Health Research Institute and Department of Microbiology, Biochemistry & Molecular Genetics, New Jersey Medical School, Rutgers Biomedical and Health Sciences, Rutgers University, Newark, NJ 07103

Running title: Redox-mechanisms of moxifloxacin lethality in *M. tb*

¶ Equal Contribution

*For correspondence: *asingh@iisc.ac.in (Amit Singh), drlicaka@njms.rutgers.edu (Karl Drlica)

Keywords: antimycobacterial, ROS, oxidative stress, moxifloxacin, fluoroquinolone, respiration, N-acetyl cysteine, redox biosensor, NADH, reductive stress, resistance

Abstract

Moxifloxacin is central to treatment of multidrug-resistant tuberculosis. Effects of moxifloxacin on *Mycobacterium tuberculosis* redox state were explored to identify strategies for increasing lethality and reducing the prevalence of extensively resistant tuberculosis. A non-invasive redox biosensor and an ROS-sensitive dye revealed that moxifloxacin induces oxidative stress correlated with *M. tuberculosis* death. Moxifloxacin lethality was mitigated by supplementing bacterial cultures with an ROS scavenger (thiourea), an iron chelator (bipyridyl), and, after drug removal, an antioxidant enzyme (catalase). Lethality was also reduced by hypoxia and nutrient starvation. Moxifloxacin increased the expression of genes involved in the oxidative stress response, iron-sulfur cluster biogenesis, and DNA repair. Surprisingly, and in contrast with *Escherichia coli* studies, moxifloxacin decreased expression of genes involved in respiration, suppressed oxygen consumption, increased the $NADH/NAD^+$ ratio, and increased the labile iron pool in *M. tuberculosis*. Lowering the $NADH/NAD^+$ ratio in *M. tuberculosis* revealed that NADH-reductive stress facilitates an iron-mediated ROS surge and moxifloxacin lethality. Treatment with N-acetyl cysteine (NAC) accelerated respiration and ROS production, increased moxifloxacin lethality, and lowered the mutant prevention concentration. Moxifloxacin induced redox stress in *M. tuberculosis* inside macrophages, and co-treatment with NAC potentiated the anti-mycobacterial efficacy of moxifloxacin during nutrient starvation, inside macrophages, and in mice where NAC restricted the emergence of resistance. Thus, oxidative stress, generated in a novel way, contributes to moxifloxacin-mediated killing of *M. tuberculosis.* The results open a way to make fluoroquinolones more effective anti-tuberculosis agents and provide a mechanistic basis for NAC-mediated enhancement of fluoroquinolone lethality *in vitro* and *in vivo.*

Author Summary

A new paradigm was revealed for stress-mediated bacterial death in which moxifloxacin treatment of *M. tuberculosis* decreases respiration rate (respiration increases in *E. coli*). Although moxifloxacin-induced, ROS-mediated bacterial death was observed, it derived from elevated levels of NADH and iron, a phenomenon not seen with antibiotic-treated *E. coli*. Nevertheless, stimulation of respiration and ROS by N-acetyl cysteine (NAC) enhanced moxifloxacin-mediated killing of *M. tuberculosis*, thereby reinforcing involvement of ROS in killing. NAC stimulation of moxifloxacin-mediated killing of *M. tuberculosis* and restriction of the emergence of resistance in a murine model of infection emphasize the importance of lethal action against pathogens. The work, plus published benefits of NAC to TB patients, encourage studies of NAC-based enhancement of fluoroquinolones.

92 **Introduction**

93 Antimicrobial resistance is a growing problem for the management of tuberculosis (TB).
94 For example, between 2009 and 2016, the number of global cases of multidrug-resistant
95 tuberculosis (MDR-TB), defined as resistance of *Mycobacterium tuberculosis* to at least
96 rifampicin and isoniazid, increased annually by over 20% (Lange et al., 2018). Additional
97 resistance to a fluoroquinolone and at least one of three injectable agents (kanamycin,
98 amikacin, or capreomycin), termed extensively drug-resistant tuberculosis (XDR-TB),
99 accounted for about 6% of MDR-TB cases in 2018 (WHO, 2019). Alarmingly, the annual
100 XDR-TB cases reported worldwide increased almost 10-fold between 2011 and 2018
101 (WHO, 2013; WHO, 2019). Increased prevalence of XDR-TB is not surprising, since the
102 fluoroquinolone-containing combination therapies used to halt progression to XDR-TB
103 utilized early quinolones (ciprofloxacin, ofloxacin, and sparfloxacin) that are only modestly
104 effective anti-TB agents (Shandil et al., 2007).

105 Efforts to find more active fluoroquinolones led to C-8 methoxy derivatives that exhibit
106 improved ability to kill *M. tuberculosis in vitro* (Dong et al., 1998). Two of these
107 compounds, moxifloxacin and gatifloxacin, have been examined as anti-TB agents (Malik
108 et al., 2006; Rodríguez et al., 2001; Ruan et al., 2016). Preclinical studies with
109 moxifloxacin in murine TB models demonstrate effective treatment with reduced relapse
110 frequency as well as treatment-shortening properties (Nuermberger et al., 2004). Indeed,
111 single-drug clinical studies indicate that the early bactericidal activity of moxifloxacin is
112 similar to that of first-line anti-TB-drugs, such as isoniazid and rifampicin. Thus,
113 moxifloxacin could be part of effective multidrug combination treatments to shorten
114 therapy time (Dorman et al., 2021; Pletz et al., 2004). Shorter treatment could increase

115 treatment compliance, further limiting the progression of MDR- to XDR-TB. However,
116 multiple phase III clinical trials have failed to corroborate the preclinical efficacy data, as
117 moxifloxacin did not shorten treatment time (Gillespie et al., 2014; Jawahar et al., 2013;
118 Jindani et al., 2014). One approach for increasing moxifloxacin efficacy is to find ways to
119 increase its lethal action.

120 The fluoroquinolones have two mechanistically distinct anti-bacterial effects: 1) they
121 block growth by forming reversible drug-gyrase-DNA complexes that rapidly inhibit DNA
122 synthesis, and 2) they kill cells (Drlica and Zhao, 2020). Death appears to arise in two
123 ways, one through chromosome fragmentation and the other through accumulation of
124 reactive oxygen species (ROS) (Drlica and Zhao, 2020). The latter appear to dominate
125 when DNA repair is proficient (Hong et al., 2020; Hong et al., 2019). We are particularly
126 interested in fluoroquinolone lethality, because *M. tuberculosis* possesses a remarkable
127 ability to evade host immune pressures (Ehrt and Schnappinger, 2009). In the absence
128 of an effective immune response, bactericidal drugs are essential for clearing infection
129 quickly. If the redox-based mechanisms of fluoroquinolone lethality seen with *E. coli*
130 extend to *M. tuberculosis,* opportunities may exist for increasing ROS and lethality,
131 thereby reducing treatment duration and increasing cure rate for MDR-TB.

132 Several methods are available for assessing the contribution of ROS to bactericidal
133 activity. Among these are direct detection of ROS levels using ROS-sensitive dyes,
134 characterization of mutants known to alter ROS levels, and examining effects of agents
135 known to suppress ROS accumulation. The present work adds detection of antibiotic-
136 induced changes in redox physiology of *M. tuberculosis* using a non-invasive, genetic
137 biosensor (Mrx1-roGFP2) (Bhaskar et al., 2014). The sensor measures the redox

138 potential (E_{MSH}) of a major mycobacterial thiol buffer, mycothiol, thereby assessing
139 oxidative effects independent of radical-sensitive fluorescent dye methods whose
140 interpretation has been debated (Dwyer et al., 2014; Liu and Imlay, 2013). Mrx1-roGFP2
141 is well-suited for this work, as it has been used to measure E_{MSH} of *M. tuberculosis* during
142 *in vitro* growth, infection of macrophages, and exposure to non-quinolone antimicrobials
143 (Bhaskar et al., 2014; Mishra et al., 2019; Mishra et al., 2017; Nambi et al., 2015).

144 In the present work, we began by asking how well *M. tuberculosis* fits the paradigm
145 for ROS-mediated killing by antimicrobials as developed from studies using *E. coli*. We
146 used moxifloxacin as a lethal stressor, because the fluoroquinolones are among the better
147 understood agents and because moxifloxacin is potentially important for tuberculosis
148 control. *M. tuberculosis* deviated markedly from *E. coli* by suppressing respiration rather
149 than increasing it during fluoroquinolone-mediated stress. That raised questions about
150 the source of ROS accumulation, since with *E. coli* ROS levels correlate with increased,
151 not decreased, respiration. We found that an increase in NADH (reductive stress)
152 accounted for the increase in ROS and lethality. When we artificially raised respiration,
153 ROS levels increased, and we observed enhanced moxifloxacin lethality *in vitro,* inside
154 macrophages, and in a murine model of infection. Raising respiration by N-acetyl cysteine
155 (NAC) treatment also reduced the emergence of resistance. Thus, the work provides a
156 mechanistic basis for developing respiration enhancers to increase the lethal action of
157 moxifloxacin and perhaps other anti-TB agents.

158 **Results**

159 **Moxifloxacin-mediated lethality associated with oxidative stress during aerobic**
160 **growth.** To obtain a reference point for *M. tuberculosis* susceptibility to moxifloxacin, we
161 determined minimal inhibitory concentration (MIC) using the resazurin microtiter assay
162 (REMA) (Padiadpu et al., 2016). MIC for moxifloxacin, which ranged from 0.125 μM to
163 0.5 μM, was similar for H37Rv and several drug-resistant isolates (Table S1; isolate
164 similarity was also seen for levofloxacin and ciprofloxacin). Thus, strain H37Rv appeared
165 to be representative and appropriate for subsequent experiments.

166 As an initial probe for moxifloxacin-induced oxidative stress, we examined a
167 derivative of *M. tuberculosis* H37Rv that expresses the redox biosensor Mrx1-roGFP2
168 (strain *Mtb*-roGFP2). This biosensor reports the redox state of the mycothiol redox couple
169 (reduced mycothiol [MSH]/oxidized mycothiol [MSSM]) in the bacterial cytosol **(Fig 1A)**
170 (Bhaskar et al., 2014). Exposure of *Mtb*-roGFP2 to hydrogen peroxide (H_2O_2) led to rapid
171 (5 min) oxidation of the biosensor in a concentration-dependent manner (Fig S1) in which
172 a 2-fold increase in the biosensor ratio represented exposure to 500 μM of H_2O_2 (Fig S1).

173 Increasing moxifloxacin concentration, up to 2.5X MIC (1X MIC = 0.5 μM) during a 48-
174 h incubation, increased the biosensor ratiometric signal by almost 2-fold (**Fig 1B,** S2A**,**
175 S2C), indicating elevated levels of oxidized mycothiol (MSSM). Above 2.5X MIC, MSSM
176 levels appeared to plateau. Measurement of ROS with CellROX Deep Red showed a
177 similar increase to 2.5X MIC moxifloxacin, followed by a plateau of mean fluorescence
178 intensity (**Fig 1C**). Moxifloxacin treatment damaged DNA and oxidized lipids (Fig S3),
179 indicating that drug-induced oxidative stress kills *M. tuberculosis* by degrading essential
180 biomolecules.

181 Maximum bacterial killing was observed at 10X MIC, a concentration at which survival
182 decreased by ≈ 2 $\log_{10}$-fold at treatment day 1 and by 6 $\log_{10}$-fold at treatment day 10 (**Fig**
183 **1D, 1E**). Survival dropped in a concentration-dependent manner, with a minimum being
184 reached at a higher concentration than observed for maximal oxidative stress (10X MIC,
185 **Fig 1B, 1C, 1D**). The discordance between the biosensor signal plateauing at 2.5X MIC
186 and killing continuing to 10X MIC (**Fig 1B**) may derive from the existence of two lethal
187 mechanisms. One mechanism, chromosome fragmentation (Dwyer et al., 2007; Malik et
188 al., 2006), likely dominates at high quinolone concentration, with an ROS-based
189 mechanism dominating at lower concentrations. Indeed, for norfloxacin treatment of *E.*
190 *coli,* oxidative effects on killing are seen only at low-to-moderate drug concentrations
191 (Malik et al., 2007). As expected, oxidative stress was not observed in *M. tuberculosis*
192 treated with sub-inhibitory concentrations of moxifloxacin (Fig S2A). The increase in
193 biosensor signal was observed as early as 12 h after initiating moxifloxacin treatment (half
194 the doubling time of untreated control cells); it then increased significantly at 48 h (Fig
195 S2A, S2B). Thus, ROS production precedes and contributes to the death of *M.*
196 *tuberculosis.* As expected, ROS levels in a moxifloxacin-resistant isolate of *M.*
197 *tuberculosis* remained low upon treatment with moxifloxacin (Fig S4A).

198 We also compared the ability of a weakly effective fluoroquinolone (ciprofloxacin, MBC
199 = 2 μM; Table S2), a moderately effective compound (levofloxacin, MBC = 1 μM), and
200 moxifloxacin (MBC = 0.5 μM) to oxidize the biosensor, all at 2.5-fold MBC. Moxifloxacin
201 induced biosensor oxidation after treatment for 12 h and 24 h (Fig S4B). In contrast,
202 ciprofloxacin did not induce biosensor oxidation, and levofloxacin triggered oxidative
203 stress only after a 24-h treatment (Fig S4B). Thus, ROS levels do not correlate with MBC,

204 a parameter obtained after long incubation time (see Discussion). The more active
205 quinolones are also more lethal at the same fold MIC with several bacterial species,
206 including mycobacteria (Dong et al., 1998; Zhao et al., 1998; Zhao et al., 1997), these
207 data corroborate the link between oxidative stress and moxifloxacin lethality.

208 High-dose chemotherapy is postulated to slow the emergence of drug resistance if the
209 drug concentration is above the mutant prevention concentration (MPC) (Drlica and Zhao,
210 2007). However bacterial strains can paradoxically show elevated survival levels at
211 extremely high drug concentrations. In the case of nalidixic acid at very high
212 concentration, *E. coli* survival can be 100% (Luan et al., 2018). Similarly, *M. tuberculosis*
213 survival increased dramatically at high moxifloxacin concentration (**Fig 1D)**.

214 Some aspects of high-concentration survival are discordant when *E. coli* and *M*.
215 *tuberculosis* are compared. For example, with *E. coli* this phenotype is associated with
216 reduced ROS levels (Luan et al., 2018); with *M*. *tuberculosis*, the biosensor and CellROX
217 signals remained high at high levels of moxifloxacin (**Fig 1B**, **1C**). This difference between
218 the organisms, which is unexplained, encouraged further comparisions.

219 **Reduction of moxifloxacin-mediated killing of *M. tuberculosis* by ROS-**
220 **mitigating agents.** Work with *E. coli* supports the idea that ROS contribute to quinolone-
221 mediated killing of bacteria (Drlica and Zhao, 2020). For example, superoxide ($O_2^{\cdot -}$)
222 damages Fe-S clusters and increases the free iron (Fe) pool (Keyer and Imlay, 1996),
223 which may then drive the generation of toxic hydroxyl radical ($HO^{\cdot}$) via the Fenton reaction
224 (Dwyer et al., 2007; Kohanski et al., 2007). To examine the effects of Fe, we assessed
225 ROS levels in *M. tuberculosis* grown in minimal medium under Fe-deficient and Fe-
226 excess conditions. Fe-overload raised ROS levels (Fig S5). Treatment with thiourea (TU),

227 a thiol-based scavenger of ROS, then reversed the Fe-induced ROS increase (Fig S5).
228 During moxifloxacin treatment of *M. tuberculosis*, a concentration-dependent increase in
229 free Fe occurs (Fig S6). Pretreatment with thiourea, at the non-toxic concentration of 10
230 mM (Nandakumar et al., 2014), increased survival of *M. tuberculosis* by almost 10-fold
231 during co-treatment with moxifloxacin (1X – 10X MIC) (**Fig 2A, 2B,** S7). These data
232 support the connection between ROS accumulation and moxifloxacin-mediated killing.

233 Another test involves chelating free ferrous Fe with bipyridyl, a high-affinity Fe^{2+}
234 chelator: with *E. coli*, bipyridyl lowers the lethal action of multiple lethal stressors (Hong
235 et al., 2017; Kohanski et al., 2007). When we treated *M. tuberculosis* cultures with a non-
236 inhibitory concentration (250 μM) of bipyridyl before moxifloxacin (**Fig 2A**), killing was
237 reduced by >100 fold (**Fig 2C**), and ROS accumulation was lowered (**Fig 2D**). Treatment
238 with bipyridyl or thiourea also protected from moxifloxacin-mediated DNA damage and
239 lipid peroxidation (Fig S3A, S3B). Collectively, the data indicate that Fe-mediated ROS
240 production is the underlying oxidative stress associated with moxifloxacin lethality.

241 Work with *E. coli* also indicates that ROS accumulates even after removal of a lethal
242 stressor (Hong et al., 2019). When we treated *M. tuberculosis* with moxifloxacin in liquid
243 medium and then plated cells on antibiotic-free 7H11 agar (see scheme, **Fig 2E**, we found
244 that addition of catalase to the agar reduced bacterial killing (**Fig 2F;** peroxide diffuses
245 freely across the cell membrane (Seaver and Imlay, 2001), allowing exogenous catalase
246 to reduce endogenous ROS levels). Replacement of catalase with 2.5% bovine serum
247 albumin, which is not expected to degrade peroxide, failed to protect *M. tuberculosis* from
248 moxifloxacin-mediated killing (Fig S8). Finding that an anti-ROS agent suppresses killing
249 after the removal of moxifloxacin indicates that the primary damage (rapid formation of

250 fluoroquinolone-gyrase-DNA complexes) can be insufficient to kill *M. tuberculosis*. Thus,
251 the post-stressor accumulation of ROS and death seen with *E. coli* occurs with *M.*
252 *tuberculosis***.**

253 We note that shorter drug-treatment times in 7H9 broth (2 days) prior to catalase
254 treatment on drug-free agar demonstrated higher survival than longer times (6 to 10
255 days), but eventually there was little difference (**Fig 2F**). A similar phenomenon has been
256 observed with *E. coli* (Hong et al., 2019). These data likely reflect ROS acting rapidly to
257 cause accelerated lethality and then having little effect on long-term killing. Overall,
258 studies with ROS-mitigating agents indicate that ROS contribute causally to quinolone-
259 mediated lethality with both *E. coli* and *M. tuberculosis*.

260 **Reduction of moxifloxacin lethality by nutrient starvation and hypoxia.** Our data
261 support previous work (Gengenbacher et al., 2010) in which nutrient starvation blocked
262 the lethal action of moxifloxacin (Loebel cidal concentration (LCC_{90}) > 32 μM) (Fig S9A,
263 S9B**,** Table S2). This phenomenon has also been reported for older quinolones with *E.*
264 *coli* (Hong et al., 2020). With *E. coli*, these effects have been attributed to a metabolic
265 shift that suppresses respiration, which is thought to be a major source of ROS.

266 Previous work (Gengenbacher et al., 2010; Wayne and Hayes, 1996) also shows that
267 hypoxic conditions reduce the lethal action of older fluoroquinolones with *M. tuberculosis*.
268 We confirmed this observation by showing that moxifloxacin-mediated killing decreases
269 significantly under hypoxic conditions (Fig S9A, S9C, Table S2). With the Wayne Cidal
270 Concentration (WCC_{90}) assay (Gengenbacher et al., 2010), the moxifloxacin
271 concentration required to kill 90% of hypoxic bacteria after 5 days of drug treatment was
272 ~10 μM (Table S2). This value corresponds to 20X MIC or 22-fold higher than the LD_{90}

273 (lethal dose) with *M. tuberculosis* (0.45 μM) cultured under aerobic growth conditions for
274 the same treatment time (Fig S10).

275 The hypoxia findings fit with moxifloxacin lethality being associated with an increase
276 in ROS, an event that should be suppessed by O_2 limitation (intracellular generation of
277 ROS may depend largely on the transfer of electrons directly to molecular O_2 (Imlay,
278 2013)). However, hypoxic suppression of moxifloxacin lethality could be due to decreased
279 respiration. To test this idea, we stimulated anaerobic respiration by providing nitrate as
280 an alternative electron acceptor (Wayne and Hayes, 1998), since that restores norfloxacin
281 lethality with anaerobic *E. coli* (Dwyer et al., 2014). Surprisingly, nitrate lowered residual
282 anaerobic lethality of moxifloxacin by several fold (Fig S9D). Nitrate was even more
283 protective with *M. tuberculosis* exposed to metronidazole (Fig S9D), an antimicrobial
284 known to be lethal in the absence of oxygen (Wayne and Sramek, 1994). The surprising
285 protective effect of nitrate, which is considered in more detail in the Discussion,
286 encouraged further comparisons with *E. coli***.**

287 **Effect of moxifloxacin on the *M. tuberculosis* transcriptome.** When we examined
288 the *M. tuberculosis* transcriptome using published data from a 16-h exposure to 2X, 4X,
289 and 8X MIC moxifloxacin (Ma et al., 2015), we found that 359 genes exhibited altered
290 expression (2-fold change across all three treatment conditions). Of these, 219 genes
291 were upregulated, and 140 were down-regulated (Dataset S1). We asked whether
292 expression after prolonged moxifloxacin exposure (16 h) is largely a secondary effect
293 from induction of other genes by comparing early changes (4-h moxifloxacin exposure) in
294 expression for a set of 28 genes deregulated at 16 h. We saw little difference (Fig S11A,

295 S11B). Thus, the patterns we observed at 16 h appear to largely reflect a primary
296 transcription response.

297 When we classified the differentially expressed genes (DEGs) according to annotated
298 functional categories (Kapopoulou et al., 2011), we found that “Information Pathways“
299 and “Insertion Sequences and Phages” were two-fold over-represented in the
300 moxifloxacin-treated *M. tuberculosis* transcriptome (Table S3). These data suggest that
301 the bacterium responds to the drug mainly by regulating DNA remodeling, transcription,
302 and translational machinery.

303 Increased expression was also seen with genes involved in redox homeostasis, such
304 as thioredoxin (*trxB1, trxB2,* and *trxC*), alkyl hydroperoxide reductase (*ahpC*), the
305 SigH/RshA system, the copper-sensing transcriptional regulator *csoR,* and the *whiB*-
306 family (*whiB4* and *whiB7*) (**Fig 3A**). Indeed, the transcriptome of moxifloxacin-treated *M.*
307 *tuberculosis* showed 67% overlap with the transcriptional signature of H_2O_2-treated cells
308 (**Fig 3B**) (Voskuil et al., 2011). Statistical analysis showed a signficant overlap between
309 the moxifloxacin transcriptome and the response to oxidative stress (H_2O_2; p = 5.39 e-14)
310 and nitrosative stress (NO; p = 2.13 e-8) (Fig S12, Table S4). An induction of oxidant-
311 responsive genes (*sox, sod, mar*) is also seen in norfloxacin-treated *E. coli* (Dwyer et al.,
312 2007). Other conditions, such as hypoxia and acidic pH, showed non-significant overlap
313 with the moxifloxacin transcriptome (Fig S12, Table S4). Collectively, the data are
314 consistent with the idea that fluoroquinolones stimulate ROS accumulation.

315 Several genes involved in repairing DNA (*recA/O/R/X, ruv ABC, uvrD, ung, dnaE2,*
316 *xthA, radA, alkA, lexA, nei, ligB*), in DNA metabolism (*nrdF2, nrdR, pyrC, pyrR*), and in
317 Fe-S cluster biogenesis (*sufR*) (Anand et al., 2021; Das et al., 2021) were also

318 upregulated (**Fig 3A**). *E. coli* treated with norfloxacin shows similar upregulation of DNA-
319 damage responses (*lexA, uvr, rec* systems and error-prone DNA polymerases IV and V),
320 nucleotide metabolism, and Fe-S cluster biogenesis (*IscRUSA*) (Dwyer et al., 2007). Such
321 results are expected from the known ability of ROS to damage DNA (Dwyer et al., 2015;
322 Foti et al., 2012).

323 With *M. tuberculosis*, moxifloxacin suppressed expression of an Fe-responsive
324 repressor (*hupB*) and an iron siderophore (*mbtF*), consistent with drug treatment
325 increasing the intrabacterial pool of labile Fe (Fig S6). Additionally, the microarray data
326 suggest that Fe–S clusters in *M. tuberculosis* are exposed to ROS during treatment with
327 moxifloxacin, resulting in Fe release from damaged clusters and increased expression of
328 Fe-S repair pathways (*sufR*). In contrast, *E. coli* upregulates Fe-uptake machinery
329 (Dwyer et al., 2007). Thus, *M. tuberculosis* and *E. coli* may generate ROS in different
330 ways.

331 In *M. tuberculosis*, moxifloxacin repressed the expression of energy-efficient
332 respiratory complexes, such as succinate dehydrogenase (*rv0248c, sdhC*), cytochrome
333 bc1 (*qcrB*), and type I NADH dehydrogenase (*nuo* operon) **(Fig 3A).** In contrast, the level
334 of the energetically inefficient, non-proton pumping *ndh2* was increased. These data
335 indicate that *M. tuberculosis* slows primary respiration and shifts to a lower energy state
336 in response to moxifloxacin. Indeed, several energy-requiring pathways (*e.g.,* cell wall
337 biosynthesis, cofactor biogenesis, cell division, transport, and ESX-secretion systems)
338 were downregulated (**Fig 3A** and Dataset S1). Moreover, genes coordinating alternate
339 carbon metabolism, such as the gluconeogenesis (*pckA*) and glyoxylate cycle (*icl1*), were
340 up-regulated (**Fig 3A**). Interestingly, Icl1 protects *M. tuberculosis* from anti-TB drugs

341 (isoniazid, rifampicin, and streptomycin), presumably by counteracting redox imbalance
342 induced by these antibiotics (Nandakumar et al., 2014). The key idea is that *M.*
343 *tuberculosis* enters into a quasi-quiescent metabolic state in response to stress from
344 moxifloxacin, opposite to fluoroquinolone effects with *E. coli* (Dwyer et al., 2014; Dwyer
345 et al., 2007).

346 **Moxifloxacin slows respiration.** As a direct test for decelerated respiration, we
347 measured the Extracellular Acidification Rate (ECAR) and Oxygen Consumption Rate
348 (OCR) for moxifloxacin-treated *M. tuberculosis* as readouts for proton-extrusion into the
349 extracellular medium (reflecting glycolysis and TCA cycle activity) and for oxidative
350 phosphorylation (OXPHOS), respectively, using a Seahorse XFp Analyzer (Lamprecht et
351 al., 2016; Mishra et al., 2019). We incubated *M. tuberculosis* in unbuffered 7H9 + glucose
352 medium in an XF microchamber, exposed the culture to 10X MIC moxifloxacin, and later
353 to the uncoupler CCCP (addition of CCCP stimulates respiration to the maximal level).
354 The difference between basal and CCCP-induced OCR estimates the spare (reserve)
355 respiratory capacity (SRC) available to counteract stressful conditions (Lamprecht et al.,
356 2016; Saini et al., 2016).

357 As expected for a growing, drug-free culture of *M. tuberculosis,* OCR showed a
358 gradual increase over the duration of the experiment (400 min); OCR increased further
359 upon uncoupling by CCCP (**Fig 4A**). In contrast, addition of 10X MIC of moxifloxacin
360 inhibited the time-dependent increase in basal OCR (**Fig 4A**), and the level of OCR upon
361 uncoupling by CCCP was markedly lower than in the absence of moxifloxacin (**Fig 4A**).
362 In parallel, we measured viability of *M. tuberculosis* and found that the bacterial culture
363 maintained 100% survival during the the entire incubation period and for an additional 4

364 h (Fig S13). Thus, the stalled oxygen-consumption effect of moxifloxacin cannot be
365 attributed to dead cells.

366 The ECAR response increased for 60 min and then gradually dropped for untreated
367 bacteria. This transient, early increase in ECAR was absent in cultures of moxifloxacin-
368 treated *M. tuberculosis*, which exhibited a greater reduction of ECAR than untreated
369 cultures at late times (**Fig 4B**). At the end of the experiment, moxifloxacin-treated cells
370 were completely exhausted of glycolytic capacity (**Fig 4B).** The slowing in OCR and
371 ECAR was also seen with treatment at lower concentrations of moxifloxacin (1X and 2.5X
372 MIC) (Fig S14), while an anti-TB drug (ethambutol) that does not generate ROS, failed to
373 significantly affect either OCR or ECAR (Fig S15).

374 In summary, moxifloxacin decelerates respiration and carbon catabolism in *M.*
375 *tuberculosis*, which likely renders the bacterium metabolically quiescent and therefore
376 less readily killed by moxifloxacin. In support of this idea, a recent study shows that
377 pretreatment with the anti-TB drugs bedaquiline (an ATP synthase inhibitor) or Q203 (a
378 cytochrome C oxidase inhibitor) reduces moxifloxacin-mediated killing of *M. tuberculosis*
379 (Lee et al., 2019).

380 **ROS derive from increased NADH.** Since moxifloxacin slows respiratory metabolism
381 (**Fig 4A**) while increasing ROS levels (**Fig 1B, 1C**), a source of ROS other than respiration
382 must exist. Slowed respiration during anoxia or chemical hypoxia places the electron
383 transport chain (ETC) in a reduced state, and NADH accumulates. This phenomenon is
384 known as reductive stress (Mavi et al., 2019). Using a redox cycling assay**,** we detected
385 an accumulation of NADH in 1X, 2.5X and 10X MIC moxifloxacin-treated *M. tuberculosis*
386 at 48 h **(Fig 5A)**. NAD^+ was raised at 1X MIC moxifloxacin, but it showed no significant

387 difference from the untreated control at lethal, elevated moxifloxacin concentrations (**Fig**
388 **5B**); the total NAD/H pool decreased at high drug concentrations (2.5X and 10X MIC; Fig
389 S16). Thus, the NADH/NAD^+ ratio increased as moxifloacin concentration increased (**Fig**
390 **5C**), indicating reductive stress.

391 We also measured NADH-reductive stress by expressing a genetically encoded, non-
392 invasive biosensor of the NADH/NAD^+ ratio (Peredox) (Bhat et al., 2016) (Fig S17). A
393 ratiometric increase in Peredox fluorescence indicated an increase in the NADH/NAD^+
394 ratio upon moxifloxacin treatment (1X to 40X MIC) at 48 h. We observed a similar
395 increase in the Peredox ratio upon treatment of *M. tuberculosis* with bedaquiline, a drug
396 known to increase the NADH/NAD^+ ratio (Fig S17) (Bhat et al., 2016). As with NADH,
397 NADPH accumulated, and the NADPH/$NADP^+$ ratio increased in response to
398 moxifloxacin treatment (Fig S18). Thus, moxifloxacin preferentially triggers NAD(P)H
399 accumulation in *M. tuberculosis***.**

400 In principle, stalled ETC and excessive reducing equivalents (NADH) can stimulate
401 ROS production in two ways. In one, NADH mobilizes bound iron, thereby increasing the
402 labile iron pool (Jaeschke et al., 1992). As previously mentioned, we found a drug-
403 concentration-dependent increase in the free iron pool in *M. tuberculosis* after
404 moxifloxacin treatment (Fig S6). Additionally, NADH autooxidation keeps iron in a
405 reduced state (Fe^{2+}); thus, NADH can drive the Fenton reaction towards hydroxyl radical
406 generation (Jaeschke et al., 1992). Second, reduced components of the electron
407 transport chain can directly transfer electrons to molecular oxygen to generate ROS
408 (Kareyeva et al., 2012; Vinogradov and Grivennikova, 2016). If these ideas are correct,

409 dissipation of the NADH overload, i.e., reductive stress, should lower the labile iron pool,
410 ROS surge, and moxifloxacin lethality.

411 We lowered the NADH/NAD^+ ratio with an *M. tuberculosis* strain that constitutively
412 expresses *Lactobacillus brevis* NADH oxidase (*Mtb-LbNox*) (**Fig 5C**, S17) (Titov et al.,
413 2016). In comparison to wild-type *M. tuberculosis*, *Mtb-LbNox* shows decreased levels of
414 NADH and increased NAD^+ without affecting the total pool of NAD^+ + NADH (**Fig 5A, 5B,**
415 **5C**, S19). As expected, moxifloxacin-treated *Mtb-LbNox* displayed a significantly reduced
416 free iron pool (Fig S6), ROS surge (**Fig 5D**), decreased DNA damage (Fig S6), and a 25-
417 to 30-fold higher surivival than wild-type cells (**Fig 5E**). Thus, increased NADH/NAD^+ ratio
418 occurring during metabolic quiescence caused by moxifloxacin accounts for the increased
419 labile iron pool, which in turn catalyzes Fenton-mediated production of ROS and cell
420 death.

421 The growth, OCR, and ECAR of *Mtb-LbNox* in 7H9 broth were the same as with wild-
422 type cells (Fig S20). Furthermore, MIC of moxifloxacin and other anti-TB drugs
423 (rifampicin, ethambutol, and bedaquiline) with *Mtb-LbNox* was similar to that of wild-type
424 *M. tuberculosis* (Table S1, S5), indicating that the interaction between drug and its
425 primary target is unaffected by overexpression of *LbNox.* In contrast, *Mtb-LbNox* exhibited
426 a 2-fold lower MIC for isoniazid, which is consistent with the interaction of isoniazid and
427 its primary target (enoyl-ACP reductase, InhA) depending on the NADH/NAD^+ ratio in *M*
428 *.tuberculosis* (Vilchèze et al., 2005). Thus, overexpression of *LbNox* appears to have no
429 effect on growth, metabolism, or respiration of *M. tuberculosis* that would complicate our
430 interpretation that NADH dissipation protects from moxifloxacin-mediated killing.

431 **N-acetyl cysteine stimulates respiration, oxidative stress, and moxifloxacin**
432 **lethality.** Previous work showed that stimulating respiration using cysteine and N-acetyl
433 cysteine (NAC) elevates the killing activity of combinations of anti-TB drugs (Vilchèze et
434 al., 2017; Vilchèze and Jacobs, 2021). Since *M. tuberculosis* responded to moxifloxacin
435 by dampening OXPHOS, we expected that countering the dampening with NAC would
436 provide a way to increase ROS further and therefore enhance moxifloxacin lethality. We
437 first measured time-dependent changes in OCR of *M. tuberculosis* upon exposure to a
438 non-toxic dose of NAC (1 mM). Addition of NAC alone produced a sharp increase in OCR
439 that reached its maximal level by 200 min (**Fig 4C**). At later times, OCR gradually
440 declined; it did not increase upon addition of CCCP (**Fig 4C**), indicating that NAC-
441 stimulated respiration exhausted the spare respiratory capacity of *M. tuberculosis*. Pre-
442 treatment with NAC reversed moxifloxacin-mediated slowing of respiration (**Fig 4D**). As
443 with NAC alone, the OCR of *M. tuberculosis,* treated with NAC plus moxifloxacin,
444 increased for 200 min and then gradually dropped; CCCP remained ineffective at
445 stimulating OCR (**Fig 4D**). These data indicate that NAC-stimulated oxygen consumption
446 by *M. tuberculosis* overcomes the dampening effect of moxifloxacin on bacterial
447 respiration.

448 Respiration, stimulated by NAC, augmented ROS accumulation upon moxifloxacin
449 treatment and increased lethality (**Fig 6A).** NAC elevated the Mrx1-roGFP2-dependent
450 redox signal for moxifloxacin-treated *M. tuberculosis*, confirming the increase in oxidative
451 stress (**Fig 6B**, S2C, S2D). We emphasize that NAC had <u>no</u> effect on moxifloxacin MIC,
452 as measured by REMA and 7H11 agar plate assay (Fig S21A, S21B); thus, the primary
453 interaction between drug and DNA gyrase (cleaved complex formation) is unaffected by

454 NAC. Supplementation of moxifloxacin at 1X and 5X MIC with 1 mM of NAC reduced
455 survival by 21- and 11-fold, respectively (**Fig 6C**), levels that are consistent with recently
456 published results using drug combinations (Vilchèze and Jacobs, 2021).

457 As a complement to the suppression of killing by addition of catalase after drug
458 removal (**Fig 2F**), we treated *M. tuberculosis* cultures with 1X and 5X MIC of moxifloxacin
459 and then plated the cells on 7H11 agar with 1 mM NAC. Post-drug addition of NAC
460 blocked formation of colonies that would otherwise have been observed (Fig S22).
461 Extended incubation (>4 weeks) resulted in the appearance of small colonies on the NAC-
462 containing plates, which was likely due to instability/oxidation of NAC ($T_{1/2}$~ 14 h) under
463 aerobic conditions (Held and Biaglow, 1994; Jaworska et al., 1999; Sommer et al., 2020).

464 NAC also potentiated moxifloxacin lethality (5- to 7-fold) with nutrient-starved, dormant
465 *M. tuberculosis* (**Fig 6D**). These data agree with recent results in which activation of
466 oxidative metabolism and respiration, through addition of L-cysteine to nutrient-starved
467 cultures, reduced the fraction of persister subpopulations and enhanced the *in vitro* lethal
468 activity of isoniazid and rifampicin (Srinivas et al., 2020). As expected, a similar treatment
469 with NAC failed to enhance moxifloxacin lethality under hypoxic conditions (**Fig 6E**),
470 consistent with NAC functioning by inducing oxygen consumption and elevating ROS
471 levels.

472 To address the effect of NAC on the acquisition of moxifloxacin resistance, we
473 measured the mutant prevention concentration (MPC) i.e., the minimal concentration of
474 moxifloxacin at which no moxifloxacin-resistant clone emerges on moxifloxacin-
475 containing 7H11 agar inoculated with ~ 2.5 x 10^9 bacteria (Drlica and Zhao, 2007; Singh
476 et al., 2017). With a clinical MDR isolate of *M. tuberculosis* (NHN1664), moxifloxacin

477 exhibited an MPC of 4 μM that was reduced to 2 μM upon co-treatment with either 1 mM
478 or 2 mM NAC. For a lower moxifloxacin concentration (1 μM, 2X MIC), the fraction of cells
479 recovered decreased by 10-fold and 100-fold when co-plated with 1 mM and 2 mM NAC,
480 respectively (Table S6). Reduction of MPC is expected when lethal activity is increased
481 (Cui et al., 2006).

482 We also addressed the possibility that some effects of NAC derived from adducts
483 formed with moxifloxacin. A series of biochemical tests (thin layer chromatography, NMR,
484 fluorescence assays, and LC-MS) revealed no evidence for adduct formation (Fig S23).

485 **Moxifloxacin-induced redox imbalance during infection of macrophages.** The
486 Mrx1-roGFP2 biosensor previously showed that first-line anti-TB drugs cause an
487 oxidative shift in the E_{MSH} of *M. tuberculosis* residing inside macrophages (Bhaskar et al.,
488 2014). When we infected macrophages with *M. tuberculosis* H37Rv or an MDR clinical
489 isolate (strain NHN1664), each expressing the biosensor Mrx1-roGFP2, *M. tuberculosis*
490 displayed redox-heterogeneity (E_{MSH}-basal [-280 mV], E_{MSH}-oxidized [-240 mV], and
491 E_{MSH}-reduced [-320 mV]); the E_{MSH}-reduced subpopulation was predominant (Bhaskar et
492 al., 2014; Mishra et al., 2019; Mishra et al., 2021) (**Fig 7A**, S24). Treatment of *M.*
493 *tuberculosis*-infected THP-1 macrophages with various concentrations of moxifloxacin
494 significantly increased the E_{MSH}-oxidized subpopulation (fuchsia colored line, **Fig 7A,**
495 S24).

496 The shift toward the E_{MSH}-oxidized redox state was seen with moderate
497 concentrations of moxifloxacin (5X MIC) at an early time point (12 h post infection), before
498 *M. tuberculosis* survival started to drop (**Fig 7A, 7B**). Thus, moxifloxacin-mediated
499 oxidative stress precedes killing: oxidative stress is not simply a consequence of cell

500 death. Bacterial survival was reduced more by higher moxifloxacin concentrations (10X
501 and 20X MIC) or longer incubation times (24 h and 48 h) (**Fig 7B**).

502 We also assessed the effect of NAC on E_{MSH} and killing of *M. tuberculosis* inside
503 macrophages. NAC itself is not cytotoxic to macrophages up to at least 5-10 mM (Amaral
504 et al., 2016; Vilchèze et al., 2017), but at those elevated concentrations it exhibits anti-
505 mycobacterial properties (Amaral et al., 2016; Cao et al., 2018). Consequently, we
506 selected non-cytotoxic, non-anti-tuberculous concentrations of NAC (1 mM and 2 mM)
507 (Amaral et al., 2016) for our test with moxifloxacin. NAC supplementation induced an
508 oxidative shift in the E_{MSH} of *M. tuberculosis* that exceeded that seen with moxifloxacin
509 alone (**Fig 7C,** S24). NAC alone had no effect on survival of *M. tuberculosis* inside THP-
510 1 macrophages; however, the NAC plus moxifloxacin combination decreased bacterial
511 burden 5-10 times more than moxifloxacin alone in both concentration- and time-
512 dependent manners (**Fig 7D**). We note that for either isoniazid or an isoniazid-rifampicin
513 combination, NAC potentiates lethality only at late times (day 6 or 7) (Vilchèze et al., 2017;
514 Vilchèze and Jacobs, 2021); NAC acts more rapidly with moxifloxacin, as the killing effect
515 is evident at days 1 and 2 (**Fig 7D**). Thus, NAC may not function in the same way with all
516 anti-TB drugs inside macrophages.

517 Moxifloxacin also lowered the level of an E_{MSH}-reduced subpopulation inside
518 macrophages (blue line, **Fig 7A**, **7C**, S24); this subpopulation was further diminished by
519 NAC supplementation. E_{MSH}-reduced subpopulations are phenotypically tolerant to anti-
520 TB drugs (Bhaskar et al., 2014; Mishra et al., 2019) and to moxifloxacin (Fig S25). Overall,
521 results with infected macrophages demonstrate that accelerating respiration and
522 oxidative metabolism by NAC can enhance moxifloxacin lethality.

523 **Potentiation of moxifloxacin lethality with NAC lowers *M. tuberculosis* burden**
524 **in a murine model of infection and restricts the emergence of resistance.** We next
525 asked whether NAC-mediated enhancement of moxifloxacin lethality occurs *in vivo*.
526 Recent work by Vilcheze *et. al.* (Vilchèze and Jacobs, 2021) directed our choice of murine
527 models: they found little enhancement by NAC on the overall lethality of a combination of
528 moxifloxacin and ethionamide when measured after long incubation using an acute model
529 of murine tuberculosis. Since ROS accelerate killing *in vitro* without increasing the extent
530 of killing (Liu et al., 2012), we shortened the drug treatment time. For this pilot test, we
531 infected BALB/c mice with the clinical MDR strain, *M. tuberculosis* NHN1664. Three
532 weeks after aerosol-mediated infection at a low dose (~100 bacilli), mice were treated
533 once daily for ten days with a low dose of moxifloxacin (50 mg/kg body weight), NAC (500
534 mg/kg body weight), or moxifloxacin plus NAC at the same doses as for mono treatments
535 (**Fig 8A**). After 10 days, moxifloxacin monotherapy reduced the bacillary load by 3-fold
536 and 100-fold in lung and spleen, respectively; NAC alone exhibited no anti-bacterial
537 activity (**Fig 8B, 8C**). The combination of moxifloxacin plus NAC reduced bacterial burden
538 by another 4- and 12-fold beyond that observed for moxifloxacin alone for lung and
539 spleen, respectively (**Fig 8B, 8C**). Thus, this preliminary finding indicates that NAC
540 stimulates the lethal action of moxifloxacin *in vivo.*

541 As a proof of concept. we also measured the effect of NAC on the selection of
542 moxifloxacin-resistant mutants in mice as described (Almeida et al., 2007; Ginsburg et
543 al., 2005). We implanted ~ 4x 10^3 *M. tuberculosis* NHN1664 in the lungs of BALB/c mice,
544 and at day 14 post-infection, when the mean lung $\log_{10}$ CFU reached ~ 10^7, mice received
545 moxifloxacin, NAC, or moxifloxacin plus NAC. After 14 days of post-treatment, 66% of

546 moxifloxacin-treated mice harbored resistant bacteria as compared to 17% when NAC
547 was also present. The combination of moxifloxacin plus NAC brought the number of
548 mutants down to the level seen with untreated animals (Table S7). Enumeration of total
549 resistant colonies confirmed that while moxifloxacin treatment increases emergence of
550 resistance, NAC supplementaion reduces the recovery of moxifloxacin-resistant mutants
551 by 8-fold (Table S7) in our pilot experiment.
552
553
554
555

556 **Discussion**

557 The experiments described above show that *M. tuberculosis* responds to moxifloxacin
558 through a lethal stress response characterized by suppressed respiration, elevated NADH
559 levels, and ROS accumulation (shown schematically in **Fig 9**). Although ROS
560 accumulation is also observed with *E. coli* during lethal stress, early steps in the *M.*
561 *tuberculosis* stress response are distinct. *M. tuberculosis* enters a metabolically quiescent
562 state characterized by increased NADH levels and $NADH/NAD^+$ ratio plus reduced
563 respiratory and glycolytic rates. This response is opposite to that seen with *E. coli* (Dwyer
564 et al., 2014; Kohanski et al., 2007; Lobritz et al., 2015). Decelerated respiration may be
565 an adaptive strategy against ROS-inducing agents produced by the host. Production of
566 ROS likely derives from increased $NADH/NAD^+$ ratio, which increases the labile, reduced
567 form of Fe to fuel the Fenton reaction. Interfering with the $NADH/NAD^+$ increase
568 dampened reductive stress and moxifloxacin lethality, suggesting that NADH disposal
569 pathways could be targeted to enhance fluoroquinolone lethality with *M. tuberculosis*.

570 **ROS contribution to lethality.** Studies with *E. coli* indicate that ROS kill bacteria by
571 damaging macromolecules *i.e.* DNA breakage, protein carbonylation, and lipid
572 peroxidation (Drlica and Zhao, 2020). Our data support the general principle that ROS
573 contribute to stress-mediated death of moxifloxacin-treated *M. tuberculosis*: 1) biosensors
574 show an increase in ROS at lethal drug concentrations, 2) iron concentrations increase
575 with moxifloxcin treatment, and 3) two ROS-mitigating agents, thiourea and bipyridyl,
576 reduce oxidative stress and killing. However, the striking increase in survival for *E. coli* at
577 very high quinolone concentrations is associated with a drop in ROS, while this is not the
578 case with *M. tuberculosis*; this difference remains unexplained.

579 Another difference is the lowering of residual fluoroquinolone lethality by nitrate with
580 hypoxic *M. tuberculosis*: the opposite is observed with norfloxacin-treated *E. coli*.
581 Previous *M. tuberculosis* work has shown that nitrate protects hypoxic bacilli from killing
582 caused by exposure to reactive nitrogen intermediates (Tan et al., 2010), acid stress (Tan
583 et al., 2010), sudden anaerobiosis (Sohaskey, 2008), or inhibition of type II NADH-
584 dehydrogenase (*ndh-2*) by thioridazine (Sohaskey, 2008). Two phenomena may
585 contribute to nitrate-mediated protection. 1) *M. tuberculosis* reduces nitrate to nitrite
586 (Cunningham-Bussel et al., 2013), which oxidizes ferrous Fe to the ferric state, thereby
587 displacing Fe from critical Fe-sulfur clusters and inducing bacteriostasis (Cunningham-
588 Bussel et al., 2013). Nitrite also remodels the *M. tuberculosis* transcriptome similar to
589 several host-imposed stresses that suppress antibiotic-mediated lethality (Cunningham-
590 Bussel et al., 2013) and ensure bacterial survival. 2) Nitrate, as a terminal electron
591 acceptor, recycles or disposes of excess reducing equivalents that accumulate during
592 anaerobic conditions (Shapleigh, 2009). Discovering strategies to halt such adaptive
593 remodeling (*e.g.,* nitrate reduction) in *M. tuberculosis* could serve as adjunct therapy for
594 moxifloxacin with hypoxic bacilli.

595 **Reductive stress as a source of ROS.** When we dissipated NADH-reductive stress
596 by overexpression of *LbNox*, the ROS surge was mitigated, and moxifloxacin lethality was
597 lowered. Production of NADH can also be lowered by stimulating the glyoxylate shunt
598 via isocitrate lyase (*icl*) – deletion of *icl* increases the lethal action of isoniazid, rifampicin,
599 and streptomycin (Nandakumar et al., 2014), suggesting that NADH-mediated ROS
600 accumulation may also contribute to the lethal action of these agents. The observed
601 increase in $NADPH/NADP^+$ ratio in response to moxifloxacin exposure could assist *M.*

602 *tuberculosis* in mitigating oxidative stress by activating NADPH-dependent antioxidant
603 systems, thioredoxins, and mycothiol. As shown by microarray data, the increase in
604 $NADPH/NADP^+$ ratio could also be a consequence of down-regulation of NADPH-
605 requiring anabolic pathways, such as polyketide/lipid biogenesis, amino acid anabolism,
606 and *de novo* nucleotide synthesis.

607 In summary, *M. tuberculosis* appears to tolerate lethal stressors of the host immune
608 system by decelerating respiration coupled with dissipation of NADH-reductive stress.
609 The need to dissipate reductive stress may be of general importance, as this type of stress
610 is also generated and amplified by hypoxia, inhibition of aerobic respiration by NO,
611 and catabolism of fatty acids (Singh et al., 2009; Voskuil et al., 2003). *M. tuberculosis*
612 dissipates reductive stress through WhiB3-mediated anabolism of polyketide lipids (Singh
613 et al., 2009). Other bacterial species also dispose of excess reductant, which they do by
614 1) using nitrate as a terminal electron acceptor during hypoxia (Tan et al., 2010), 2) fueling
615 fermentation under nitrosative stress (Richardson et al., 2008), and 3) secreting
616 phenazines (redox-active polyketides) that generate NAD^+ from NADH (Price-Whelan et
617 al., 2007). Moxifloxacin is the first anti-mycobacterial agent shown to stimulate NADH-
618 reductive stress.

619 **Lethality enhancement by N-acetyl cysteine**. Vilchèze and Jacobs (Vilchèze and
620 Jacobs, 2021) reported that NAC boosts the lethality of anti-TB drug combinations *in vitro*.
621 We emphasize that a general, enhancing effect on drug-target interactions by NAC is
622 unlikely, because such effects are usually detected by MIC measurement (Drlica and
623 Zhao, 2020): NAC has no effect on moxifloxacin MIC. This observation reinforces the
624 concept that drug-target interactions are mechanistically distinct from downstream ROS-

625 based killing (protection from killing, which is called tolerance when no change in MIC
626 occurs, is distinct from resistance, which is measured as an increase in MIC).

627 To simplify interpretation of killing data, we focused on a single drug, moxifloxacin,
628 rather than drug combinations. Previous demonstration that NAC stimulates respiration
629 (Vilchèze and Jacobs, 2021) made it a useful tool for examining killing mechanism. NAC
630 increased moxifloxacin-mediated ROS accumulation and lethality with cultured *M.*
631 *tuberculosis*. Increased killing was initially surprising, because NAC has anti-oxidant
632 properties expected to reduce moxifloxacin lethality (Ezeriņa et al., 2018). It is likely that
633 the effect of NAC depends on the level of stress, since with other bacterial species, genes
634 (*mazF, cpx, lepA*) and treatments (chemical generation of superoxide, H_2O_2) are known
635 to be protective at low levels of stress but destructive at high ones (Dorsey-Oresto et al.,
636 2013; Li et al., 2014; Mosel et al., 2013; Rodríguez-Rojas et al., 2020). Indeed, treatment
637 with a sub-lethal concentration of H_2O_2 activates the OxyR-regulon in *E. coli* and "primes"
638 the bacterium to conteract subsequent oxidative-stress challenge. At higher
639 concentrations, H_2O_2 is cidal (Imlay and Linn, 1986). With the high level of stress
640 produced by moxifloxacin, the respiration-stimulating activity of NAC dominates and adds
641 to ROS derived from NADH-reductive stress.

642 As expected from *in vitro* studies, NAC increased moxifloxacin lethality with infected
643 macrophages and mice. The kinetic effects of ROS explain why our short-term treatment
644 model with infected mice showed stimulation by NAC, while the longer treatment used
645 previously with antimicrobial combinations did not (Vilchèze and Jacobs, 2021).

646 We addressed the potential of NAC to suppress the emergence of resistance by
647 measuring its effect on MPC. Although MPC is a bacteriostatic parameter (MIC of the

648 least susceptible mutant subpopulation), highly lethal agents lower it in an animal model
649 of infection, presumably by killing mutants (Cui et al., 2006). Thus, we were not surprised
650 that stimulation of moxifloxacin lethality by NAC lowered MPC. In a murine infection
651 model, NAC reduced the recovery of resistant mutants by 8-fold.

652 Although MPC for moxifloxacin is lower than concentrations achieved in serum by
653 approved doses (Dong et al., 2000), the clinical situation is likely complex: moxifloxacin
654 shows poor penetration into caseous regions of tubercular granulomas in a rabbit model
655 of experimental tuberculosis (Prideaux et al., 2015; Sarathy et al., 2019). Low, local
656 moxifloxacin concentrations may promote the emergence of fluoroquinolone resistance
657 (Davies Forsman et al., 2020). Thus, NAC supplementation could increase the probability
658 that moxifloxacin concentration is above MPC in vivo, but additional work is required to
659 test this idea.

660 NAC is a potential candidate as a lethality enhancer, because it is relatively safe for
661 humans (it has been used to alleviate drug-induced toxicity in TB-patients (Baniasadi et
662 al., 2010; Kranzer et al., 2015)). Furthermore, NAC by itself exhibits anti-mycobacterial
663 activity inside macrophages, mice, and guinea pigs (Amaral et al., 2016; Palanisamy et
664 al., 2011), and a small clinical trial in which NAC was administered to TB patients
665 improved host health, immunological response, and early sputum conversion
666 (Mahakalkar et al., 2017; Nagrale et al., 2013). The present work provides a mechanistic
667 foundation for refining NAC-based enhancement of anti-tuberculosis agents. Assessing
668 the general clinical significance of ROS enhancement is also complex, because ROS
669 accelerates killing without lowering bacterial survival at long incubations. This
670 phenomenon has been observed with *S. aureus* (Liu et al., 2012), *E. coli* (Hong et al.,

671 2019), and *M. tuberculosis* (**Fig. 2F**; S4B). With *M. tuberculosis*-infected mice, NAC
672 stimulates reduction of bacterial load at short but not long incubation times (Vilchèze and
673 Jacobs, 2021). Thus, an appropriate dosing interval must be determined, initially guided
674 by *in vitro* pharmacodynamic studies (Almeida et al., 2007; Firsov et al., 2003; Ginsburg
675 et al., 2005; Gumbo et al., 2004). Relevant tissue concentrations of NAC and moxifloxacin
676 for various doses over time must also be determined before clinical relevance can be
677 assessed. The present report, plus that of Vilchèze and Jacobs (Vilchèze and Jacobs,
678 2021), encourage such followup work.

679 **Materials and Methods**

680 **Bacterial strains and culture conditions.** *M. tuberculosis* H37Rv and drug-
681 resistant clinical isolates JAL 1934, JAL 2287, JAL 2261, and BND 320 were kind gifts
682 from Dr. Kanury V.S. Rao (International Centre for Genetic Engineering and
683 Biotechnology, Delhi, India). MDR strain NHN1664, originally isolated in China, was
684 obtained from BEI Resources, NIAID, NIH. Strain *Mtb*-roGFP2 was generated by
685 transforming *M. tuberculosis* strain H37Rv with an *E. coli*-mycobacterial shuttle vector,
686 pMV762 (Singh et al., 2006; Steyn et al., 2003). Plasmid pMV762 contains the Mrx1-
687 roGFP2 biosensor construct under control of the *M. tuberculosis hsp60* promoter and a
688 hygromycin-resistance gene as a selection marker. Hygromycin (MP Biomedical, cat. No.
689 0219417091, Santa Ana, CA) was used at a final concentration of 50 µg/mL. Plasmid
690 (pGMCgS-0×-Ptb38-LbNOX-FLAG-SD1) containing a *lbnox* construct was kind gift from
691 Dr. Dirk Schnappinger and Dr. Sabine Ehrt (Weill Cornell Medicine, New York, USA).
692 Plasmid was electroporated into wild-type *M. tuberculosis* H37Rv to create the *Mtb-*
693 *LbNox* strain. Streptomycin was used at a final concentration of 25 µg/mL. Plasmid

694 pMV762-Peredox-mcherry was a kind gift from Dr. Ashwani Kumar (Council of
695 Scientific and Industrial Research, Institute of Microbial Technology, Chandigarh , India).
696 All strains, including laboratory *M. tuberculosis* strain H37Rv and *M. tuberculosis*
697 expressing the Mrx1-roGFP2 redox biosensor, were grown in 7H9 broth supplemented
698 with 0.2% glycerol, 0.05% Tween-80, and ADS (0.5% albumin, 0.2% dextrose, and
699 0.085% NaCl) with shaking at 180 RPM in a rotary shaker incubator (Lab Therm LT-X;
700 Kuhner, Basel, Switzerland) or on 7H11 agar supplemented with ADS or OADC (ADS
701 plus 0.05% oleic acid and 0.004% catalase (Sigma Aldrich, cat. No. C9322, St Louis, MO)
702 or ADC (ADS plus 0.004% catalase) at 37°C. Bacterial strains expressing Mrx1-roGFP2
703 were grown in media containing hygromycin.
704 **Determination of minimal inhibitory concentration (MIC) under aerobic growth**
705 **conditions.** MIC was determined by a resazurin microtiter assay (REMA) using 96-well
706 flat-bottom plates (Padiadpu et al., 2016). *M. tuberculosis* strains were cultured in
707 7H9+ADS medium (Bhaskar et al., 2014) and grown to exponential phase (OD_{600} = 0.4
708 to 0.8). Approximately 1×10^5 bacteria per well were added in a total volume of 200 µL of
709 7H9+ADS medium. Wells lacking *M. tuberculosis* served as controls. Additional controls
710 consisted of wells containing cells without drug treatment (growth control). After 5 days
711 of incubation at 37°C in the presence of fluoroquinolone (or NAC), 30 µL of 0.02%
712 resazurin (Sigma-Aldrich, cat. No. R7017, St Louis, MO) was added, and plates were
713 incubated for an additional 24 h. Fluorescence intensity was measured using a
714 SpectraMax M3 plate reader (Molecular Devices, San Jose, CA) in the bottom-reading
715 mode with excitation at 530 nm and emission at 590 nm. Percent inhibition was calculated
716 from the relative fluorescence units compared with an untreated control culture; MIC was

717 taken as the lowest drug concentration that resulted in at least 90% reduction in
718 fluorescence compared to the untreated growth control.

719 **Determination of bacterial survival.** To determine the number of viable bacilli,
720 aliquots were removed from cultures, cells were concentrated by centrifugation (4200 *g*,
721 5 min) to remove drug or treatment compounds, and they were resuspended in an equal
722 volume of medium. Ten-fold dilutions were prepared, and 20 µL aliquots were spotted on
723 drug-free 7H11 agar plates containing 10% ADC or ADS. Plates were incubated for 3-4
724 weeks at 37°C for CFU enumeration by visual inspection.

725 Concentration-kill curves were obtained by treating exponentially growing cultures of
726 *M. tuberculosis* (OD_{600} of 0.3 or ≈ 5×10^7 cells/mL) with various concentrations of
727 moxifloxacin. Tubes were incubated with shaking at 180 RPM for 10 days at 37°C.
728 Aliquots were taken at various intervals, serially diluted, and plated on drug-free agar for
729 CFU enumeration.

730 LD_{90} (lethal dose) for moxifloxacin under *in vitro,* aerobic-culture conditions was
731 measured by treating 10-mL cultures in 50-mL centrifuge tubes under aerobic conditions
732 (shaking at 180 RPM, 37°C), followed by CFU measurement. A 90% reduction in CFU
733 on treatment day 5, compared with the input control, was defined as LD_{90}.

734 To determine the effect of an Fe-chelator on moxifloxacin-mediated lethality, 250 µM
735 (a non-inhibitory concentration) of bipyridyl (Sigma-Aldrich, cat.no. D216305, St Louis,
736 MO) was added to bacterial cultures 15 min prior to moxifloxacin addition; bipyridyl was
737 present throughout the experiment (i.e., 10 days).

738 For experiments with thiourea or N-acetyl cysteine (NAC), thiourea (10 mM) or NAC
739 (1 mM) was added 1 h prior to moxifloxacin and was maintained for 2 days or 10 days.

740 Aliquots were taken at indicated times, serially diluted, and plated for CFU enumeration
741 on drug-free agar.

742 **Post-stressor bactericidal activity of moxifloxacin.** *M. tuberculosis* cultures were
743 treated with moxifloxacin for 48 h, the drug was removed by washing, and cells were
744 plated on drug-free 7H11 agar with or without 1 mM NAC or with 2.5% bovine serum
745 albumen (BSA), followed by visual CFU determination.

746 **Measurement of E_{MSH} using the Mrx1-roGFP2 redox biosensor.** For intra-
747 mycobacterial E_{MSH} determination during *in-vitro* growth or during *ex-vivo* macrophage-
748 infection conditions, strain *Mtb*-roGFP2 was grown in 7H9 broth or in THP-1
749 macrophages, respectively. Cultures were then treated with moxifloxacin, and at various
750 times they were treated with 10 mM N-ethylmaleimide (NEM; Sigma-Aldrich, cat. No.-
751 E3876, St Louis, MO) for 5 min at room temperature followed by fixation with 4%
752 paraformaldehyde (PFA; Himedia, cat. No. GRM3660, Mumbai, India) for 1 h at room
753 temperature. Bacilli or infected macrophages were analyzed using a FACSVerse Flow
754 cytometer (BD Biosciences, San Jose, CA). Intramycobacterial E_{MSH} was determined
755 using the Nernst Equation as described previously (Bhaskar et al., 2014). E_{MSH} is defined
756 as the standard reduction potential of the MSH/MSSM redox couple (reduced mycothiol
757 to oxidized mycothiol.

758 The biosensor response was measured by analyzing the fluorescence ratio at a fixed
759 emission (510 nm) after excitation at 405 and 488 nm. Data were analyzed using the BD
760 FACSuite software. These ratiometric data were normalized to measurements with cells
761 treated with 10 mM cumene hydroperoxide (Sigma-Aldrich- cat. No. 247502, St Louis,
762 MO), which reports maximal oxidation of the biosensor, and 20 mM dithiothreitol (Sigma-

763 Aldrich, cat. No. D9779, St Louis, MO), which reports maximal reduction. 10,000 events
764 per sample were analyzed.

765 **ROS measurement using CellROX Deep Red.** Cultures of exponentially growing *M.*
766 *tuberculosis* at an initial OD_{600} of 0.3 were treated with various concentrations of
767 moxifloxacin for 48 h. Sterile 50 mL-capacity polypropylene centrifuge tubes (Abdos, cat
768 no. P10404, Roorkee, India), containing 10 mL of culture, were incubated in a shaker
769 incubator (180 RPM, 37°C). Then cells were harvested by centrifugation (4200 *g* for 5
770 min) and resuspended in 100 µL of growth medium. As per manufacturer's instructions,
771 CellROX Deep Red (Invitrogen, cat. No. C10422, Waltham, MA) was added to a final
772 concentration of 5 µM, and cells were agitated on a rocker (Biobee Tech, Bangalore,
773 India) for 30 min. After incubation, cells were washed to remove residual dye by
774 centrifugation (4200 *g* for 5 min). Cells were resuspended in 300 uL phosphate-buffered
775 saline, pH 7.4) and then fixed by addition of 4% paraformaldehyde (PFA) for 1 h at room
776 temperature. Fluorescence was measured at a fixed emission (670 nm) after excitation
777 with a red laser (640 nm) using a BD FACSVerse Flow cytometer (BD Biosciences, San
778 Jose, CA) with 10,000 events per sample. No autofluorescence was observed.

779 **Determination of DNA damage by TUNEL assay.** DNA damage was measured by
780 using In Situ Cell Death Detection Kit, TMR red (Roche Molecular Biochemicals,
781 Indianapolis, IN, Cat. No.- 12156792910), which is based on TUNEL (TdT-mediated
782 dUTP-X nick end labeling) assay (Fan et al., 2018; Vilchèze et al., 2013). An equal
783 number of cells (based on OD_{600}) were taken at various times of treatment with
784 moxifloxacin, washed once by centrifugation, and fixed in 2% paraformaldehyde (PFA).
785 PFA was removed by washing cells, followed by resuspension in 2% sodium dodecyl

786 sulfate (SDS) and a second wash by centrifugation. DNA double-strand breaks were
787 labeled in 100 µl of TUNEL reaction mix for 3-4 h. Cells incubated with label solution only
788 (no terminal transferase) were used as negative controls. Fluorescence was measured
789 at a fixed emission (585 nm) after excitation with green-yellow laser (561 nm) using a BD
790 FACSAria Flow cytometer (BD Biosciences, San Jose, CA). 10,000 events were acquired
791 per sample.

792 **Lipid Peroxidation Assay.** Cultures were grown to mid-log phase (OD_{600}= 0.6-0.8).
793 Lipid hydroperoxides were quantified from cell pellets after centrifugation (4000 *g,* 5 min),
794 using FOX2 reagent (Nambi et al., 2015). Briefly, cell pellets were resuspended in 1:2
795 chloroform/methanol and mixed by vortexing. Next, chloroform and water were added at
796 a 1:1 mixture The samples were then centrifuged to separate the water and organic
797 phases. The organic phase was collected and washed twice with water. 200 µl of the
798 organic phase was incubated with 1 ml of FOX2 reagent in the dark for 1 h at 22°C. Lipid
799 hydroperoxides were measured spectrophotometrically at 560 nm and normalized to
800 culture turbidity (OD_{600}).

801 **Macrophage preparation and infection by *M. tuberculosis*.** The human monocytic
802 cell line THP-1 was grown in RPMI1640 medium (Cell Clone, Manassas, VA)
803 supplemented with 10% heat-treated (55°C) fetal bovine serum (MP Biomedical, cat. no.
804 092916754, Santa Ana, CA). A total of 3×10^5 cells/well was seeded into a 24-well cell-
805 culture plate. THP-1 monocytes were stimulated to differentiate into macrophage-like
806 cells by treatment with 20 ng/mL phorbol 12-myristate 13-acetate (PMA; Sigma-Aldrich
807 Co., St Louis, MO) for 18-20 h at 37°C and incubated further for 48 h to allow
808 differentiation (Bhaskar et al., 2014). The resulting macrophage-like cells were infected

809 with *Mtb*-roGFP2 or MDR *M. tuberculosis* NHN1664 expressing Mrx1-roGFP2 at a
810 multiplicity of infection (MOI) of 10 and incubated for 4 h at 37 °C in 5% CO_2. After
811 Infection, extracellular bacteria were removed by washing three times (by centrifugation)
812 with phosphate-buffered saline (PBS; 137 mM NaCl, 2.7 mM KCl, 10 mM Na_2HPO_4, and
813 1.4 mM KH_2PO_4, pH 7.4). Moxifloxacin (Sigma-Aldrich, cat. No. PHR1542, St Louis, MO),
814 with or without NAC (Sigma-Aldrich, cat. No. A7250, St Louis, MO), was added to infected
815 cells that were incubated for various times. For CFU determination, infected cells were
816 lysed in 7H9 medium containing 0.06% sodium dodecyl sulfate (SDS); dilutions were
817 prepared using 7H9 medium, and aliquots were plated on 7H11+OADC agar plates
818 (Bhaskar et al., 2014). Plates were incubated at 37 °C for 3-4 weeks before colonies were
819 counted.

820 **Nutrient starvation.** Starvation was achieved as previously described
821 (Gengenbacher et al., 2010). Briefly, cultures of *M. tuberculosis* H37Rv were grown to
822 exponential phase in roller-culture bottles (Corning, cat no.- 430518, Corning, NY)
823 containing Middlebrook 7H9 medium, supplemented with ADS and 0.05 % Tween 80, at
824 37°C with rolling at 6 RPM in a roller incubator (120 Vac Roll-In Incubator; Wheaton,
825 Millville, NJ). Cultures grown to $OD_{600} \approx 0.2$ were harvested by centrifugation (4000 *g* for
826 5 min) followed by two washes with phosphate-buffered saline (PBS; pH 7.4)
827 supplemented with 0.025 % Tween 80 (PBST). Bacterial cells were diluted to a final OD_{600}
828 of 0.1 in PBS. 50 mL of this suspension was transferred into a roller-culture bottle and
829 incubated for 14 days to achieve starvation conditions.

830 **Hypoxia.** For determination of moxifloxacin lethality under hypoxic conditions,
831 bacterial cultures ($OD_{600} = 0.1$) were placed in Vacutainer tubes (Becton Dickinson, cat.

832 no. 367812, Franklin Lakes, NJ) followed by incubation for 14-21 days at 37°C (Taneja
833 and Tyagi, 2007). A high cell density (OD_{600} = 0.1) was used for rapid achievement of
834 hypoxia, which was observed as decolorization of methylene blue (final concentration
835 was 1.5 μg/mL) in the culture medium. When hypoxia was established, moxifloxacin was
836 added to cultures anaerobically. Metronidazole at 10 mM and isoniazid at 10 μM were
837 used as positive and negative controls, respectively. Drugs were injected in volumes of
838 100 μL in phosphate-buffered saline following passage of argon through the drug solution
839 to remove residual oxygen. Hypoxic cultures were treated with drugs for five days, similar
840 to the incubation time for MIC determination with aerobically growing cells. After
841 treatment, Vacutainer tubes were unsealed, and end-point bacterial survival was
842 determined by plating on drug-free agar, incubating for 3-4 weeks at 37°C, and visually
843 enumerating colonies.

844 **Effect of nitrate on survival of hypoxic bacteria.** Survival during nitrate-dependent
845 respiration was achieved by supplementing *M. tuberculosis* cultures with 5 mM sodium
846 nitrate. Nitrate was added when cultures were placed in Vacutainer tubes before hypoxia.
847 All other conditions were as described above for hypoxia.

848 **Microarray data analysis.** Gene expression data from GSE71200 (Gene Expression
849 Omnibus, NCBI or GEO) was used for analyzing the response of *M. tuberculosis* to
850 moxifloxacin (Ma et al., 2015). The data were expressed as a two-channel microarray
851 with control and drug-exposed *M. tuberculosis* stained with Cy3 and Cy5 dyes,
852 respectively. We used GSM1829746, GSM1829747, and GSM1829748, which consist of
853 published data for *M. tuberculosis* exposed to 2X, 4X, or 8X MIC (1X MIC = 0.4 μM) of
854 moxifloxacin for 16 h. Normalized expression data for GSE71200 was downloaded from

855 GEO (Barrett et al., 2013; Edgar et al., 2002), and probe IDs were mapped to the
856 respective gene-IDs. The expression levels for genes having multiple probes were
857 averaged, and genes lacking data were removed from further analysis. Differentially
858 expressed genes (DEGs) were defined as genes that were upregulated or downregulated
859 by at least 2-fold in all 3 moxifloxacin treatment conditions.

860 For overlap analysis of differentially expressed genes in moxifloxacin-exposed
861 bacteria compared with other stress-induced conditions ($\log_2$ fold change >1 or <-1; p <
862 0.01 are considered differentially expressed genes in stress conditions), GeneOverlap
863 (v1.22.0) package from R (v3.6.3) was used (Core-Team, 2018; Li and Sinai, 2019). It
864 uses Fisher's exact test to find statistical significance by calculating the p-value and the
865 odds ratio for the overlap (p-value < 0.05 and an odds ratio of > 1 were taken as the
866 significance thresholds).

867 **OCR and ECAR measurements.** To measure basal oxygen consumption rate (OCR)
868 and extracellular acidification rate (ECAR), log-phase *M. tuberculosis* cultures (OD_{600}=
869 0.6-0.8) were briefly (one day) incubated in 7H9 medium containing the non-
870 metabolizable detergent tyloxapol (MP Biomedical, cat. No.157162, Santa Ana, CA) and
871 lacking ADS or a carbon source. These cultures were then passed 10 times through a
872 26-gauge syringe needle followed by centrifugation at 100 *g* for 1-2 mins to remove
873 clumps of bacterial cells. The resulting single-cell suspensions of bacteria at 2×10^6
874 cells/well were placed in the bottom of wells of a Cell-Tak (Corning, cat. No. 354240,
875 Corning, NY)-coated XF culture plate (Agilent/Seahorse Biosciences, Santa Clara, CA).
876 Measurements were performed using a Seahorse XFp analyzer (Agilent/Seahorse
877 Biosciences, Santa Clara, CA) with cells in unbuffered 7H9 growth medium (pH 7.35

878 lacking monopotassium phosphate and disodium phosphate) containing glucose (2
879 mg/mL) as a carbon source. OCR and ECAR measurements were recorded for ~21 min
880 (3 initial baseline readings) before addition of moxifloxacin (1X, 2.5X or 10X MIC; 1X MIC
881 = 0.5 μM), which was delivered automatically through the drug ports of the sensor
882 cartridge (Wave Software, Agilent Technologies, Santa Clara, CA). NAC or CCCP was
883 similarly added through drug ports at times indicated in figures. OCR and ECAR were
884 measured for an additional 6 h in the absence or presence of moxifloxacin and/or NAC.
885 Changes in OCR and ECAR readings triggered by moxifloxacin were calculated as a
886 percentage of the third baseline reading for OCR and ECAR taken prior to drug injection.
887 **ROS measurement under Fe-depletion conditions.** Iron starvation was as
888 described previously (Kurthkoti et al., 2017). Briefly, log-phase *M. tuberculosis* cultures
889 were grown in minimal medium (0.5% (wt/vol) asparagine, 0.5% (wt/vol) KH_2PO4, 2%
890 glycerol, 0.05% Tween 80, 10% ADS, 0.5 mg/L of sterile $ZnCl_2$, 0.1 mg/ L of $MnSO_4$, and
891 40 mg/L of $MgSO_4$) to early stationary phase (OD_{600} of ~1). To remove metal ions, the
892 minimal medium was treated with 5% Chelex-100 (Bio-Rad, cat. No. 142-2842, Hercules,
893 CA) for 24 h with gentle agitation. This Fe-depleted culture was diluted further to OD_{600}
894 of 0.1 in the same medium and allowed to grow to early stationary phase to deplete stored
895 Fe. The Fe-depleted cells were further treated with 50 μg/ml of freshly prepared
896 deferoxamine mesylate (Sigma Aldrich, cat. No. D9533, St Louis, MO)-containing minimal
897 medium for 6 days. The cells were washed and diluted in minimal medium containing 80
898 μM $FeCl_3$ or 80 μM $FeCl_3$ + 10 mM thiourea for an additional 4 days. ROS was quantified
899 by CellROX Deep Red dye using Flow cytometry as described in the section titled ROS
900 measurement using CellROX Deep Red.

901 **Cellular Fe Estimation.** Cell-free Fe levels were measured using the ferrozine-based
902 assay as described previously (Fish, 1988; Vilchèze et al., 2017). Briefly, *M. tuberculosis*
903 cultures were grown to an OD_{600} of 0.3-0.4 followed by treatment with 0X, 1X, 2.5X, or
904 10X MIC of moxifloxacin. After 48 h of treatment, cells were harvested and washed twice
905 with ice-cold PBS. The cell pellets were resuspended in 1 mL of 50 mM NaOH and lysed
906 using a bead beater. The cell lysate sample (300 µl) was mixed with 10 mM HCl (300 µL)
907 followed by addition of Fe-detection reagent (6.5 mM Ferrozine, 6.5 mM Neocuproine, 1
908 M ascorbic acid, and 2.5 M ammonium acetate in water) (90 µl). The reaction mix was
909 incubated at 37°C for 30 min, and then absorbance at 562 nm was measured. The cellular
910 Fe concentration was determined by plotting the absorbance values against a standard
911 curve of $FeCl_3$ concentration gradient and normalized to protein content. Protein
912 concentration was determined using the Pierce BCA Protein Assay Kit (Thermo Scientific,
913 cat. no. 23225, Rockford, IL).

914 **Estimation of NAD^+, $NADP^+$, NADH, and NADPH.** *M. tuberculosis* H37Rv was grown
915 to OD_{600} ~0.35 and treated with 1X, 2.5X or 10X MIC of moxifloxacin for 48 h. Pyridine
916 nucleotide levels were determined by a redox-cycling assay (Chawla et al., 2012; Singh
917 et al., 2009). Protein concentration of NAD^+ or NADH extracts was determined using the
918 Pierce BCA Protein Assay Kit (Thermo Scientific, cat. no. 23225, Rockford, IL) to
919 normalize NAD(P)H and $NAD(P)^+$ concentrations.

920 **Analysis of mixtures containing moxifloxacin plus and minus NAC by thin layer**
921 **chromatography (TLC).** Thin-layer chromatography (TLC) was performed using silica
922 gel 60 GF_{254} precoated aluminium backed plates (0.25 mm thickness; Merck, Darmstadt,
923 Germany), and visualization was accomplished by irradiation with UV light at 254 nm.

924 Stock solutions of moxifloxacin (10 mM) and NAC (0.2 M, 2 M and 20 M) were prepared
925 independently in DMSO and phosphate buffer (PB, pH 7.4, 10 mM), respectively. In a
926 typical incubation, moxifloxacin (100 μL at a final concentration of 2 mM) was
927 independently reacted with various concentrations of NAC (5 μL, final concentration 2
928 mM, 20 mM, or 200 mM) in 395 μL PB (pH 7.4, 10 mM). In a control experiment,
929 moxifloxacin (100 μL, final concentration 2 mM) was added to 400 μL PB (pH 7.4, 10
930 mM). The mixtures were incubated at 37 ºC on an Eppendorf ThermoMixer Comfort (800
931 rpm). The reactions were monitored by spotting aliquots (5 μL) from the incubation
932 mixtures onto the TLC plate at designated times. The solvent system used was MeOH
933 and $CHCl_3$ (1:9).

934 **Analysis of mixtures containing moxifloxacin plus and minus NAC by NMR.**
935 Deuterated phosphate buffer (PB, 10 mM) was prepared by dissolving monobasic
936 potassium phosphate (KH_2PO_4, 4 mg) and dibasic potassium phosphate (K_2HPO_4, 12
937 mg) in deuterated water (D_2O), and the pH was adjusted to 7.4 using 40% (w/w) sodium
938 deuteroxide solution in D_2O (Sigma-Aldrich, cat. No. 151882, St Louis, MO). Stock
939 solutions of moxifloxacin (10 mM) and NAC (0.2 M) were prepared in DMSO and
940 deuterated phosphate buffer (PB, pH 7.4, 10 mM) respectively. In a typical reaction,
941 moxifloxacin (200 μL, 2 mM final concentration) was incubated with NAC (10 μL, 2 mM
942 final concentration) in 790 μL deuterated PB (pH 7.4, 10 mM). In a control experiment,
943 moxifloxacin (200 μL, 2 mM final concentration) was added to 800 μL deuterated PB (pH
944 7.4, 10 mM). The incubation mixtures were incubated at 37 ºC in an Eppendorf
945 ThermoMixer Comfort (800 rpm). An aliquot (0.5 mL) of the incubation mixture was taken
946 after 1 h of incubation, and ^{1}H NMR and ^{19}F NMR spectra were recorded. ^{1}H NMR was

947 acquired with 64 scans on a Jeol 400 MHz spectrometer using deuterated water (D_2O;
948 Sigma-Aldrich) as an internal standard. Chemical shifts (δ) were reported in ppm
949 downfield from D_2O (δ = 4.79 ppm) for ^1H NMR. ^{19}F spectra was recorded on a JEOL (376
950 MHz) using an external reference (α, α, α-trifluorotoluene, δ_F = -63.72 ppm).

951 **Fluorescence-based detection of intracellular levels of moxifloxacin in wild-**
952 **type *M. smegmatis*.** Stock solutions of moxifloxacin (0.05 mM) and NAC (200 mM) were
953 prepared in DMSO and phosphate buffer (pH 7.4, 10 mM), respectively. Wild-type *M.*
954 *smegmatis* cultures were grown in Middlebrook 7H9 broth supplemented with glycerol
955 (0.2%) and Tween-80 (0.1%). Exponential-phase cultures of wild-type *M. smegmatis,*
956 grown to OD_{600} of 0.3 (985 µL), were transferred to 1.5 mL Eppendorf tubes and either
957 left untreated or treated with NAC (5 µL, final concentration 1 mM) for 1 h prior to addition
958 of 2x MIC of moxifloxacin (10 µL, final concentration 0.5 µM). Treated cells were
959 incubated with shaking at 180 rpm in a rotary shaker incubator at 37 °C for 48 h. The cell
960 suspension was then centrifuged at 9,391 *g* at 4 °C for 15 min, and the pellet was washed
961 twice with 1x phosphate buffer saline (PBS) and resuspended in 1 mL PBS in a
962 microcentrifuge tube. The cells were lysed by sonication using a 130-watt ultrasonic
963 processor (Vx 130W) by stepping a microtip with a 4 min pulse on-time (with 3s ON and
964 3s OFF pulse, 60% amplitude, 20 kHz frequency) under ice-cold conditions. An aliquot
965 (100 µL) of whole-cell lysate was withdrawn from the above samples and dispensed into
966 a 96-well microtiter plate. Fluorescence ascribed to moxifloxacin (λ_{ex} = 289 nm and λ_{em} =
967 488 nm), recovered in NAC-untreated or-pretreated *M. smegmatis* lysates, was recorded
968 using an Ensight Multimode Plate Reader (PerkinElmer, India). Readings were collected
969 from the top with 25 flashes per well and with a focus height adjusted to 9.5 mm.

970 **Intracellular levels of moxifloxacin in *M. smegmatis* using LC/MS.** Stock
971 solutions of moxifloxacin (0.05 mM) and NAC (200 mM) were prepared as described
972 above. Whole-cell lysates of wild-type *M. smegmatis* treated with moxifloxacin (0.5 μM,
973 2x MIC) plus or minus NAC (1 mM) were prepared as described in the fluorescence-
974 based method employed for the detection of moxifloxacin. An aliquot (100 μL) of whole-
975 cell lysate was withdrawn from the incubation mixtures, diluted with methyl alcohol (100
976 μL), and centrifuged at 9,390 x *g* at 4 °C for 15 min. The supernatant fluids (50 μL) were
977 removed, diluted with methyl alcohol (50 μL), and analyzed by LC/MS. All measurements
978 were performed using the positive ion mode with high-resolution, multiple reaction
979 monitoring (MRM-HR) analysis with a Sciex X500R quadrupole time-of flight (QTOF)
980 mass spectrometer fitted with an Exion UHPLC system having a Kinetex 2.6 mm
981 hydrophilic interaction liquid chromatography (HILIC) column (100 Å particle size, 150
982 mm length, and 3 mm internal diameter; Phenomenex, Intek Chromasol Pvt. Ltd., India).
983 Nitrogen was used as the nebulizer gas, with nebulizer pressure set at 50 psi. MS was
984 calibrated in the positive mode, and samples were analyzed with the following
985 parameters: Mode: electrospray ionization (ESI), ion source gas 1 = 40 psi, ion source
986 gas 2 = 50 psi, curtain gas = 30, CAD gas = 7, spray voltage = 5500 V, and temperature
987 = 500 °C. The MRM-HR mass spectrometry parameters were moxifloxacin (Q1, $M + H^+$)
988 = 402.18, moxifloxacin-NAC adduct (Q2, $M + H^+$) = 565.21, declustering potential = 80
989 V, collision energy = 20 V, collision exit potential = 5 V, and accumulation time = 0.24 s.
990 The LC runs were for 30 min with a gradient of 100% solvent A (0.1% HCOOH in water)
991 for 5 min, linear gradient of solvent B (acetonitrile 0% to 100%) for 25 min followed by
992 100% solvent A for 5 min, all at a flow rate of 0.5 mL per min.

993 **Determination of Mutant Prevention Concentration (MPC).** MPC of moxifloxacin
994 with *M. tuberculosis* NHN1664 was determined by methods described previously (Dong
995 et al., 2000; Singh et al., 2017). Cultures of MDR strain *M. tuberculosis* NHN1664 were
996 grown to OD_{600} 0.6-0.7. Approximately 2.5×10^9 bacilli were plated on 7H11 agar
997 containing either moxifloxacin (2X, 4X, or 8X MIC) alone or in combination with NAC at
998 either 1 mM or 2 mM. Resistant colonies were enumerated after incubation at 37°C for 8
999 weeks. The drug-resistant phenotype was confirmed by replating on drug-containing
1000 7H11-agar plates. MPC was determined as the lowest concentration of drug that
1001 prevented bacterial colony formation when $>2\times10^9$ bacteria were plated on drug-
1002 containing 7H11 plates. Mutation frequency with moxifloxacin was calculated as the
1003 number of mutants appearing on drug-containing plates divided by the viable input
1004 bacteria.

1005 **Determination of drug-tolerant *M. tuberculosis* population *ex vivo.*** Murine bone-
1006 marrow-derived macrophages (BMDMs) were infected with Mrx1-roGFP2-expressing *M.*
1007 *tuberculosis* H37Rv at a multiplicity of infection of 10. After washing off extracellular
1008 bacteria, infected macrophages were left untreated for 24 h for the emergence of the
1009 drug-tolerant population. At 24 h post-infection, macrophages harbouring E_{MSH}-reduced
1010 and E_{MSH}-basal *M. tuberculosis* were sorted using BD FACS Aria™ Fusion Flow
1011 Cytometer. The sorted, infected BMDM cells were seeded into 96-well plates followed by
1012 treatment with 3X MIC of moxifloxacin (1X MIC = 0.5 μM) for 48 h. After treatment, cells
1013 were lysed with 0.05% sodium dodecyl sulfate (SDS) in 7H9 medium, serially diluted, and
1014 plated on 7H11-OADC agar plates. Plates were incubated at 37˚C for 3-4 weeks before
1015 colony forming units (CFUs) were enumerated.

1016 ***In vivo* drug efficacy.** All animal studies were executed as per guidelines prescribed
1017 by the Committee for the Purpose of Control and Supervision of Experiments on Animals,
1018 Government of India, with approval from the Institutional Animal Ethical Committee and
1019 Biosafety Level-3 Committee. 6- to 8-week-old female pathogen-free BALB/c mice were
1020 infected via a low-dose aerosol exposure to the *M. tuberculosis* MDR strain NHN1664
1021 using a Madison chamber aerosol generation instrument. The short-course mouse model
1022 of infection was performed as described previously (Lenaerts et al., 2003). At day one
1023 post infection, three mice were sacrificed to verify implantation of ∼100 CFU of bacteria
1024 per mouse. Mice were randomly divided into 4 groups (n = 5 per group). Feed and water
1025 were given *ad libitum*. Treatment with moxifloxacin and/or NAC started 21 days post-
1026 infection and continued for 10 days; untreated control mice received water rather than the
1027 two test compounds. Treated mice were administered moxifloxacin (50 mg/kg of body
1028 weight), NAC (500 mg/ kg of body weight) and a combination of moxifloxacin and NAC at
1029 50 mg/kg and 500 mg/kg body weight, respectively, by oral gavage, once daily. Five
1030 infected mice were sacrificed at the start of treatment as pretreatment controls. After
1031 treatment, mice were sacrificed, and the lungs and spleen were harvested for
1032 measurement of bacterial burden. CFUs were determined by plating appropriate serial
1033 dilutions on 7H11 (supplemented with OADC) agar plates and counting visible colonies
1034 after 3–4 weeks of incubation at 37˚C. Data were normalized to whole organ.

1035 **Detection of moxifloxacin-resistant mutants in murine model of infection.** 6- to
1036 8-week-old female, pathogen-free BALB/c mice were infected via a high-dose aerosol
1037 exposure to the *M. tuberculosis* MDR strain NHN1664 using a Madison chamber aerosol
1038 generation instrument. At day one post infection, three mice were sacrificed to determine

1039 implantation of >10^3 CFU of bacteria per mouse. Mice were then randomly divided into
1040 4 treatment groups, with 6 mice each in the vehicle control group, NAC-only group, groups
1041 receiving either moxifloxacin or a combination of NAC and moxifloxacin. Feed and water
1042 were given *ad libitum*. Treatment with moxifloxacin and/or NAC started 14 days post-
1043 infection and continued for 14 days; untreated control mice received water rather than the
1044 two test compounds. Treated mice were administered moxifloxacin (50 mg/kg of body
1045 weight), NAC (500 mg/ kg of body weight) and a combination of moxifloxacin and NAC at
1046 50 mg/kg and 500 mg/kg body weight, respectively, by oral gavage, once daily. 5 infected
1047 mice were sacrificed at the start of treatment as pre-treatment controls. After treatment,
1048 mice were sacrificed, and the lungs and spleen were harvested together. Moxifloxacin-
1049 resistant mutants were selected by plating the undiluted homogenates (lung+spleen) on
1050 five 7H11 plates containing 0.5 μM of moxifloxacin (4X MIC). Plates were incubated for
1051 3–4 weeks at 37˚C.

1052 **Statistical analysis.** Statistical analysis was performed using GraphPad Prism
1053 version 8.4.3 software. Mean and standard deviation values were plotted as indicated in
1054 figure legends. A *p*-value of less than 0.05 was considered significant. Statistical
1055 significance was determined by unpaired two-tailed student's t-test; either one-way or
1056 two-way ANOVA was performed where comparison of multiple groups was made.

1057

1058 **Acknowledgements**

1059 We thank the following for critical comments on the manuscript: Lanbo Shi, Bo
1060 Shopsin, and Xilin Zhao.

1061 **Declaration**

The funders had no role in study design, data collection and analysis, decision to publish, or preparation of the manuscript. The authors have declared that no competing interests exist.

1072 **References**

1073 Almeida, D., E. Nuermberger, S. Tyagi, W.R. Bishai, and J. Grosset. 2007. *In vivo*
1074 validation of the mutant selection window hypothesis with moxifloxacin in a murine
1075 model of tuberculosis. *Antimicrob. Agents Chemother.* 51:4261-4266.

1076 Amaral, E.P., E.L. Conceição, D.L. Costa, M.S. Rocha, J.M. Marinho, M. Cordeiro-
1077 Santos, M.R. D'Império-Lima, T. Barbosa, A. Sher, and B.B. Andrade. 2016. N-
1078 acetyl-cysteine exhibits potent anti-mycobacterial activity in addition to its known
1079 anti-oxidative functions. *BMC Microbiol.* 16:251.

1080 Anand, K., A. Tripathi, K. Shukla, N. Malhotra, A.K. Jamithireddy, R.K. Jha, S.N.
1081 Chaudhury, R.S. Rajmani, A. Ramesh, V. Nagaraja, B. Gopal, G. Nagaraju, A.S.
1082 Narain Seshayee, and A. Singh. 2021. *Mycobacterium tuberculosis* SufR responds
1083 to nitric oxide via its 4Fe–4S cluster and regulates Fe–S cluster biogenesis for
1084 persistence in mice. *Redox Biol.* 46:102062.

1085 Baniasadi, S., P. Eftekhari, P. Tabarsi, F. Fahimi, M.R. Raoufy, M.R. Masjedi, and A.A.
1086 Velayati. 2010. Protective effect of N-acetylcysteine on antituberculosis drug-
1087 induced hepatotoxicity. *Eur. J. Gastroenterol. Hepatol.* 22:1235-1238.

1088 Barrett, T., S.E. Wilhite, P. Ledoux, C. Evangelista, I.F. Kim, M. Tomashevsky, K.A.
1089 Marshall, K.H. Phillippy, P.M. Sherman, M. Holko, A. Yefanov, H. Lee, N. Zhang,
1090 C.L. Robertson, N. Serova, S. Davis, and A. Soboleva. 2013. NCBI GEO: archive
1091 for functional genomics data sets--update. *Nucleic Acids Research* 41:D991-D995.

1092 Bhaskar, A., M. Chawla, M. Mehta, P. Parikh, P. Chandra, D. Bhave, D. Kumar, K.S.
1093 Carroll, and A. Singh. 2014. Reengineering redox sensitive GFP to measure
1094 mycothiol redox potential of *Mycobacterium tuberculosis* during infection. *PLoS*
1095 *Pathog.* 10:e1003902.

1096 Bhat, S.A., I.K. Iqbal, and A. Kumar. 2016. Imaging the NADH:NAD+ homeostasis for
1097 understanding the metabolic response of mycobacterium to physiologically
1098 relevant stresses. *Frontiers in Cellular and Infection Microbiology* 6:
1099 Cao, R., G. Teskey, H. Islamoglu, R. Abrahem, S. Munjal, K. Gyurjian, L. Zhong, and V.
1100 Venketaraman. 2018. Characterizing the effects of glutathione as an
1101 immunoadjuvant in the treatment of tuberculosis. *Antimicrob. Agents Chemother.*
1102 62:e01132-01118.
1103 Chawla, M., P. Parikh, A. Saxena, M. Munshi, M. Mehta, D. Mai, A.K. Srivastava, K.V.
1104 Narasimhulu, K.E. Redding, N. Vashi, D. Kumar, A.J.C. Steyn, and A. Singh. 2012.
1105 *Mycobacterium tuberculosis* WhiB4 regulates oxidative stress response to
1106 modulate survival and dissemination *in vivo*. *Mol. Microbiol.* 85:1148-1165.
1107 Core-Team, R. 2018. A language and environment for statistical computing. R foundation
1108 for statistical computing. Vienna, Austria. In.
1109 Cui, J., Y. Liu, R. Wang, W. Tong, K. Drlica, and X. Zhao. 2006. The mutant selection
1110 window in rabbits infected with *Staphylococcus aureus*. *J. Infect. Dis.* 194:1601-
1111 1608.
1112 Cunningham-Bussel, A., T. Zhang, and C.F. Nathan. 2013. Nitrite produced by
1113 *Mycobacterium tuberculosis* in human macrophages in physiologic oxygen
1114 impacts bacterial ATP consumption and gene expression. *Proc. Natl. Acad. Sci.*
1115 *U.S.A.* 110:E4256-4265.
1116 Das, M., A. Dewan, S. Shee, and A. Singh. 2021. The multifaceted bacterial cysteine
1117 desulfurases: From metabolism to pathogenesis. *Antioxidants (Basel)* 10:

1118 Davies Forsman, L., K. Niward, J. Kuhlin, X. Zheng, R. Zheng, R. Ke, C. Hong, J.
1119 Werngren, J. Paues, U.S.H. Simonsson, E. Eliasson, S. Hoffner, B. Xu, J.-W.
1120 Alffenaar, T. Schön, Y. Hu, and J. Bruchfeld. 2020. Suboptimal moxifloxacin and
1121 levofloxacin drug exposure during treatment of patients with multidrug-resistant
1122 tuberculosis: results from a prospective study in China. *Eur. Respir. J.* 57:2003463.
1123 Dong, Y., C. Xu, X. Zhao, J. Domagala, and K. Drlica. 1998. Fluoroquinolone action
1124 against mycobacteria: Effects of C-8 substituents on growth, survival, and
1125 resistance. *Antimicrob. Agents Chemother.* 42:2978-2984.
1126 Dong, Y., X. Zhao, B.N. Kreiswirth, and K. Drlica. 2000. Mutant prevention concentration
1127 as a measure of antibiotic potency: studies with clinical isolates of *Mycobacterium*
1128 *tuberculosis*. *Antimicrob. Agents Chemother.* 44:2581-2584.
1129 Dorman, S.E., P. Nahid, E.V. Kurbatova, P.P.J. Phillips, K. Bryant, K.E. Dooley, M. Engle,
1130 S.V. Goldberg, H.T.T. Phan, J. Hakim, J.L. Johnson, M. Lourens, N.A. Martinson,
1131 G. Muzanyi, K. Narunsky, S. Nerette, N.V. Nguyen, T.H. Pham, S. Pierre, A.E.
1132 Purfield, W. Samaneka, R.M. Savic, I. Sanne, N.A. Scott, J. Shenje, E. Sizemore,
1133 A. Vernon, Z. Waja, M. Weiner, S. Swindells, and R.E. Chaisson. 2021. Four-
1134 month rifapentine regimens with or without moxifloxacin for tuberculosis. *N. Engl.*
1135 *J. Med.* 384:1705-1718.
1136 Dorsey-Oresto, A., T. Lu, M. Mosel, X. Wang, T. Salz, K. Drlica, and X. Zhao. 2013. *YihE*
1137 kinase is a central regulator of programmed cell death in bacteria. *Cell Reports*
1138 3:528-537.
1139 Drlica, K., and X. Zhao. 2007. Mutant selection window hypothesis updated. *Clin. Infect.*
1140 *Dis.* 44:681-688.

1141 Drlica, K., and X. Zhao. 2020. Bacterial death from treatment with fluoroquinolones and
1142 other lethal stressors. *Expert Rev. Anti Infect. Ther.* 1-18.
1143 Dwyer, D.J., P.A. Belenky, J.H. Yang, I.C. MacDonald, J.D. Martell, N. Takahashi, C.T.Y.
1144 Chan, M.A. Lobritz, D. Braff, E.G. Schwarz, J.D. Ye, M. Pati, M. Vercruysse, P.S.
1145 Ralifo, K.R. Allison, A.S. Khalil, A.Y. Ting, G.C. Walker, and J.J. Collins. 2014.
1146 Antibiotics induce redox-related physiological alterations as part of their lethality.
1147 *Proc. Natl. Acad. Sci. U.S.A.* 111:E2100-E2109.
1148 Dwyer, D.J., J.J. Collins, and G.C. Walker. 2015. Unraveling the physiological
1149 complexities of antibiotic lethality. *Annu. Rev. Pharmacol. Toxicol.* 55:313-332.
1150 Dwyer, D.J., M.A. Kohanski, B. Hayete, and J.J. Collins. 2007. Gyrase inhibitors induce
1151 an oxidative damage cellular death pathway in *Escherichia coli*. *Mol. Syst. Biol.*
1152 3:91-91.
1153 Edgar, R., M. Domrachev, and A.E. Lash. 2002. Gene Expression Omnibus: NCBI gene
1154 expression and hybridization array data repository. *Nucleic Acids Research*
1155 30:207-210.
1156 Ehrt, S., and D. Schnappinger. 2009. Mycobacterial survival strategies in the phagosome:
1157 defence against host stresses. *Cellular Microbiology* 11:1170-1178.
1158 Ezeriņa, D., Y. Takano, K. Hanaoka, Y. Urano, and T.P. Dick. 2018. N-Acetyl Cysteine
1159 functions as a fast-acting antioxidant by triggering intracellular H_2S and sulfane
1160 sulfur production. *Cell Chem. Biol.* 25:447-459.e444.
1161 Fan, X.Y., B.K. Tang, Y.Y. Xu, A.X. Han, K.X. Shi, Y.K. Wu, Y. Ye, M.L. Wei, C. Niu, K.W.
1162 Wong, G.P. Zhao, and L.D. Lyu. 2018. Oxidation of dCTP contributes to antibiotic

1163 lethality in stationary-phase mycobacteria. *Proc. Natl. Acad. Sci. U.S.A.*
1164 201719627.
1165 Firsov, A.A., S.N. Vostrov, I.Y. Lubenko, K. Drlica, Y.A. Portnoy, and S.H. Zinner. 2003.
1166 In vitro pharmacodynamic evaluation of the mutant selection window hypothesis
1167 using four fluoroquinolones against *Staphylococcus aureus*. *Antimicrob. Agents*
1168 *Chemother.* 47:1604-1613.
1169 Fish, W.W. 1988. Rapid colorimetric micromethod for the quantitation of complexed iron
1170 in biological samples. *Methods Enzymol.* 158:357-364.
1171 Foti, J.J., B. Devadoss, J.A. Winkler, J.J. Collins, and G.C. Walker. 2012. Oxidation of the
1172 guanine nucleotide pool underlies cell death by bactericidal antibiotics. *Science*
1173 336:315-319.
1174 Gengenbacher, M., S.P. Rao, K. Pethe, and T. Dick. 2010. Nutrient-starved, non-
1175 replicating *Mycobacterium tuberculosis* requires respiration, ATP synthase and
1176 isocitrate lyase for maintenance of ATP homeostasis and viability. *Microbiology*
1177 *(Reading)* 156:81-87.
1178 Gillespie, S.H., A.M. Crook, T.D. McHugh, C.M. Mendel, S.K. Meredith, S.R. Murray, F.
1179 Pappas, P.P.J. Phillips, and A.J. Nunn. 2014. Four-month moxifloxacin-based
1180 regimens for drug-sensitive tuberculosis. *N. Engl. J. Med.* 371:1577-1587.
1181 Ginsburg, A.S., R. Sun, H. Calamita, C.P. Scott, W.R. Bishai, and J.H. Grosset. 2005.
1182 Emergence of fluoroquinolone resistance in *Mycobacterium tuberculosis* during
1183 continuously dosed moxifloxacin monotherapy in a mouse model. *Antimicrob.*
1184 *Agents Chemother.* 49:3977-3979.

1185 Gumbo, T., A. Louie, M.R. Deziel, L.M. Parsons, M. Salfinger, and G.L. Drusano. 2004.
1186 Selection of a moxifloxacin dose that suppresses drug resistance in
1187 *Mycobacterium tuberculosis*, by use of an in vitro pharmacodynamic infection
1188 model and mathematical modeling. *J. Infect. Dis.* 190:1642-1651.
1189 Held, K.D., and J.E. Biaglow. 1994. Mechanisms for the oxygen radical-mediated toxicity
1190 of various thiol-containing compounds in cultured mammalian cells. *Radiat. Res.*
1191 139:15-23.
1192 Hong, Y., L. Li, G. Luan, K. Drlica, and X. Zhao. 2017. Contribution of reactive oxygen
1193 species to thymineless death in *Escherichia coli*. *Nat. Microbiol.* 2:1667-1675.
1194 Hong, Y., Q. Li, Q. Gao, J. Xie, H. Huang, K. Drlica, and X. Zhao. 2020. Reactive oxygen
1195 species play a dominant role in all pathways of rapid quinolone-mediated killing. *J.*
1196 *Antimicrob. Chemother.* 75:576-585.
1197 Hong, Y., J. Zeng, X. Wang, K. Drlica, and X. Zhao. 2019. Post-stress bacterial cell death
1198 mediated by reactive oxygen species. *Proc. Natl. Acad. Sci. U.S.A.* 116:10064-
1199 10071.
1200 Imlay, J.A. 2013. The molecular mechanisms and physiological consequences of
1201 oxidative stress: lessons from a model bacterium. *Nat. Rev. Microbiol.* 11:443-454.
1202 Imlay, J.A., and S. Linn. 1986. Bimodal pattern of killing of DNA-repair-defective or
1203 anoxically grown Escherichia coli by hydrogen peroxide. *J Bacteriol* 166:519-527.
1204 Jaeschke, H., C. Kleinwaechter, and A. Wendel. 1992. NADH-Dependent reductive stress
1205 and ferritin-bound iron in allyl alcohol-induced lipid peroxidation *in vivo*: The
1206 protective effect of vitamin E. *Chem. Biol. Interact.* 81:57-68.

1207 Jawahar, M.S., V.V. Banurekha, C.N. Paramasivan, F. Rahman, R. Ramachandran, P.
1208 Venkatesan, R. Balasubramanian, N. Selvakumar, C. Ponnuraja, A.S. Iliayas, N.P.
1209 Gangadevi, B. Raman, D. Baskaran, S.R. Kumar, M.M. Kumar, V. Mohan, S.
1210 Ganapathy, V. Kumar, G. Shanmugam, N. Charles, M.R. Sakthivel, K. Jagannath,
1211 C. Chandrasekar, R.T. Parthasarathy, and P.R. Narayanan. 2013. Randomized
1212 clinical trial of thrice-weekly 4-month moxifloxacin or gatifloxacin containing
1213 regimens in the treatment of new sputum positive pulmonary tuberculosis patients.
1214 *PLoS One* 8:e67030.
1215 Jaworska, M., G. Szulińska, M. Wilk, and J. Tautt. 1999. Capillary electrophoretic
1216 separation of N-acetylcysteine and its impurities as a method for quality control of
1217 pharmaceuticals. *J. Chromatogr. A* 853:479-485.
1218 Jindani, A., T.S. Harrison, A.J. Nunn, P.P.J. Phillips, G.J. Churchyard, S. Charalambous,
1219 M. Hatherill, H. Geldenhuys, H.M. McIlleron, S.P. Zvada, S. Mungofa, N.A. Shah,
1220 S. Zizhou, L. Magweta, J. Shepherd, S. Nyirenda, J.H. van Dijk, H.E. Clouting, D.
1221 Coleman, A.L.E. Bateson, T.D. McHugh, P.D. Butcher, and D.A. Mitchison. 2014.
1222 High-dose rifapentine with moxifloxacin for pulmonary tuberculosis. *N. Engl. J.*
1223 *Med.* 371:1599-1608.
1224 Kapopoulou, A., J.M. Lew, and S.T. Cole. 2011. The MycoBrowser portal: a
1225 comprehensive and manually annotated resource for mycobacterial genomes.
1226 *Tuberculosis (Edinb)* 91:8-13.
1227 Kareyeva, A.V., V.G. Grivennikova, and A.D. Vinogradov. 2012. Mitochondrial hydrogen
1228 peroxide production as determined by the pyridine nucleotide pool and its redox
1229 state. *Biophys. Acta Bioenerg.* 1817:1879-1885.

1230 Keyer, K., and J.A. Imlay. 1996. Superoxide accelerates DNA damage by elevating free-
1231 iron levels. *Proc. Natl. Acad. Sci. U.S.A.* 93:13635-13640.
1232 Kohanski, M.A., D.J. Dwyer, B. Hayete, C.A. Lawrence, and J.J. Collins. 2007. A common
1233 mechanism of cellular death induced by bactericidal antibiotics. *Cell* 130:797-810.
1234 Kranzer, K., W.F. Elamin, H. Cox, J.A. Seddon, N. Ford, and F. Drobniewski. 2015. A
1235 systematic review and meta-analysis of the efficacy and safety of N-acetylcysteine
1236 in preventing aminoglycoside-induced ototoxicity: implications for the treatment of
1237 multidrug-resistant TB. *Thorax* 70:1070-1077.
1238 Kurthkoti, K., H. Amin, M.J. Marakalala, S. Ghanny, S. Subbian, A. Sakatos, J. Livny,
1239 S.M. Fortune, M. Berney, and G.M. Rodriguez. 2017. The capacity of
1240 *Mycobacterium tuberculosis* to survive iron starvation might enable it to persist in
1241 iron-deprived microenvironments of human granulomas. *mBio* 8:
1242 Lamprecht, D.A., P.M. Finin, M.A. Rahman, B.M. Cumming, S.L. Russell, S.R. Jonnala,
1243 J.H. Adamson, and A.J.C. Steyn. 2016. Turning the respiratory flexibility of
1244 *Mycobacterium tuberculosis* against itself. *Nat. Comm.* 7:12393.
1245 Lange, C., D. Chesov, J. Heyckendorf, C.C. Leung, Z. Udwadia, and K. Dheda. 2018.
1246 Drug-resistant tuberculosis: An update on disease burden, diagnosis and
1247 treatment. *Respirology* 23:656-673.
1248 Lee, B.S., N.P. Kalia, X.E.F. Jin, E.J. Hasenoehrl, M. Berney, and K. Pethe. 2019.
1249 Inhibitors of energy metabolism interfere with antibiotic-induced death in
1250 mycobacteria. *J. Biol. Chem.* 294:1936-1943.

1251 Lenaerts, A.J., V. Gruppo, J.V. Brooks, and I.M. Orme. 2003. Rapid *in vivo* screening of
1252 experimental drugs for tuberculosis using gamma interferon gene-disrupted mice.
1253 *Antimicrob. Agents Chemother.* 47:783-785.
1254 Li, L., Y. Hong, G. Luan, M. Mosel, M. Malik, K. Drlica, and X. Zhao. 2014. Ribosomal
1255 elongation factor 4 promotes cell death associated with lethal stress. *mBio*
1256 5:e01708.
1257 Li, S., and M. Sinai. 2019. GeneOverlap: Test and visualize gene overlaps. In.
1258 Liu, Y., and J.A. Imlay. 2013. Cell death from antibiotics without the involvement of
1259 reactive oxygen species. *Science* 339:1210-1213.
1260 Liu, Y., X. Liu, Y. Qu, X. Wang, L. Li, and X. Zhao. 2012. Inhibitors of reactive oxygen
1261 species accumulation delay and/or reduce the lethality of several
1262 antistaphylococcal agents. *Antimicrob. Agents Chemother.* 56:6048-6050.
1263 Lobritz, M.A., P. Belenky, C.B.M. Porter, A. Gutierrez, J.H. Yang, E.G. Schwarz, D.J.
1264 Dwyer, A.S. Khalil, and J.J. Collins. 2015. Antibiotic efficacy is linked to bacterial
1265 cellular respiration. *Proc. Natl. Acad. Sci. U.S.A.* 112:8173.
1266 Luan, G., Y. Hong, K. Drlica, and X. Zhao. 2018. Suppression of reactive oxygen species
1267 accumulation accounts for paradoxical bacterial survival at high quinolone
1268 concentration. *Antimicrob. Agents Chemother.* 62:e01622-01617.
1269 Ma, S., K.J. Minch, T.R. Rustad, S. Hobbs, S.L. Zhou, D.R. Sherman, and N.D. Price.
1270 2015. Integrated Modeling of Gene Regulatory and Metabolic Networks in
1271 Mycobacterium tuberculosis. *PLoS Comput. Biol.* 11:e1004543.
1272 Mahakalkar, S.M., D. Nagrale, S. Gaur, C. Urade, B. Murhar, and A. Turankar. 2017. N-
1273 acetylcysteine as an add-on to Directly Observed Therapy Short-I therapy in fresh

1274 pulmonary tuberculosis patients: A randomized, placebo-controlled, double-
1275 blinded study. *Perspect Clin. Res.* 8:132-136.
1276 Malik, M., S. Hussain, and K. Drlica. 2007. Effect of anaerobic growth on quinolone
1277 lethality with *Escherichia coli*. *Antimicrob. Agents Chemother.* 51:28-34.
1278 Malik, M., X. Zhao, and K. Drlica. 2006. Lethal fragmentation of bacterial chromosomes
1279 mediated by DNA gyrase and quinolones. *Mol. Microbiol.* 61:810-825.
1280 Mavi, P.S., S. Singh, and A. Kumar. 2019. Reductive stress: New insights in physiology
1281 and drug tolerance of mycobacterium. *Antioxid. Redox Signal.* 32:1348-1366.
1282 Mishra, R., S. Kohli, N. Malhotra, P. Bandyopadhyay, M. Mehta, M. Munshi, V. Adiga,
1283 V.K. Ahuja, R.K. Shandil, R.S. Rajmani, A.S.N. Seshasayee, and A. Singh. 2019.
1284 Targeting redox heterogeneity to counteract drug tolerance in replicating
1285 *Mycobacterium tuberculosis*. *Sci. Transl. Med.* 11:eaaw6635.
1286 Mishra, R., V. Yadav, M. Guha, and A. Singh. 2021. Heterogeneous host–pathogen
1287 encounters coordinate antibiotic resilience in *Mycobacterium tuberculosis*. *Trends*
1288 *in Microbiology* 29:606-620.
1289 Mishra, S., P. Shukla, A. Bhaskar, K. Anand, P. Baloni, R.K. Jha, A. Mohan, R.S. Rajmani,
1290 V. Nagaraja, N. Chandra, and A. Singh. 2017. Efficacy of β-lactam/β-lactamase
1291 inhibitor combination is linked to WhiB4-mediated changes in redox physiology of
1292 *Mycobacterium tuberculosis*. *eLife* 6:
1293 Mosel, M., L. Li, K. Drlica, and X. Zhao. 2013. Superoxide-mediated protection of
1294 *Escherichia coli* from antimicrobials. *Antimicrob. Agents Chemother.* 57:5755-
1295 5759.

1296 Nagrale, D., S. Mahakalkar, and S. Gaur. 2013. Supplementation of N-acetylcysteine as
1297 an adjuvant in treatment of newly diagnosed pulmonary tuberculosis patients: A
1298 prospective, randomized double blind, placebo controlled study. *Eur. Respir. J.*
1299 42:P2833.
1300 Nambi, S., J.E. Long, B.B. Mishra, R. Baker, K.C. Murphy, A.J. Olive, H.P. Nguyen, S.A.
1301 Shaffer, and C.M. Sassetti. 2015. The oxidative stress network of *Mycobacterium*
1302 *tuberculosis* reveals coordination between radical detoxification systems. *Cell Host*
1303 *Microbe* 17:829-837.
1304 Nandakumar, M., C. Nathan, and K.Y. Rhee. 2014. Isocitrate lyase mediates broad
1305 antibiotic tolerance in *Mycobacterium tuberculosis*. *Nature Communications*
1306 5:4306.
1307 Nuermberger, E.L., T. Yoshimatsu, S. Tyagi, R.J. O'Brien, A.N. Vernon, R.E. Chaisson,
1308 W.R. Bishai, and J.H. Grosset. 2004. Moxifloxacin-containing regimen greatly
1309 reduces time to culture conversion in murine tuberculosis. *Am. J. Respir. Crit. Care*
1310 *Med.* 169:421-426.
1311 Padiadpu, J., P. Baloni, K. Anand, M. Munshi, C. Thakur, A. Mohan, A. Singh, and N.
1312 Chandra. 2016. Identifying and tackling emergent vulnerability in drug-resistant
1313 mycobacteria. *ACS Infectious Diseases* 2:592-607.
1314 Palanisamy, G.S., N.M. Kirk, D.F. Ackart, C.A. Shanley, I.M. Orme, and R.J. Basaraba.
1315 2011. Evidence for oxidative stress and defective antioxidant response in guinea
1316 pigs with tuberculosis. *PLoS One* 6:e26254.

1317 Pletz, M.W.R., A. De Roux, A. Roth, K.-H. Neumann, H. Mauch, and H. Lode. 2004. Early
1318 bactericidal activity of moxifloxacin in treatment of pulmonary tuberculosis: A
1319 prospective, randomized study. *Antimicrob. Agents Chemother.* 48:780.
1320 Price-Whelan, A., L.E.P. Dietrich, and D.K. Newman. 2007. Pyocyanin alters redox
1321 homeostasis and carbon flux through central metabolic pathways in *Pseudomonas*
1322 *aeruginosa* PA14. *J. Bacteriol.* 189:6372-6381.
1323 Prideaux, B., L.E. Via, M.D. Zimmerman, S. Eum, J. Sarathy, P. O'Brien, C. Chen, F.
1324 Kaya, D.M. Weiner, P.-Y. Chen, T. Song, M. Lee, T.S. Shim, J.S. Cho, W. Kim,
1325 S.N. Cho, K.N. Olivier, C.E. Barry, and V. Dartois. 2015. The association between
1326 sterilizing activity and drug distribution into tuberculosis lesions. *Nat. Med.*
1327 21:1223-1227.
1328 Richardson, A.R., S.J. Libby, and F.C. Fang. 2008. A nitric oxide-inducible lactate
1329 dehydrogenase enables *Staphylococcus aureus* to resist innate immunity. *Science*
1330 319:1672.
1331 Rodríguez-Rojas, A., J.J. Kim, P.R. Johnston, O. Makarova, M. Eravci, C. Weise, R.
1332 Hengge, and J. Rolff. 2020. Non-lethal exposure to H_2O_2 boosts bacterial survival
1333 and evolvability against oxidative stress. *PLoS Genet.* 16:e1008649.
1334 Rodríguez, J.C., M. Ruiz, A. Climent, and G. Royo. 2001. *In vitro* activity of four
1335 fluoroquinolones against *Mycobacterium tuberculosis*. *Int. J. Antimicrob. Agents*
1336 17:229-231.
1337 Ruan, Q., Q. Liu, F. Sun, L. Shao, J. Jin, S. Yu, J. Ai, B. Zhang, and W. Zhang. 2016.
1338 Moxifloxacin and gatifloxacin for initial therapy of tuberculosis: a meta-analysis of
1339 randomized clinical trials. *Emerg. Microbes Infect.* 5:e12-e12.

1340 Saini, V., Bridgette M. Cumming, L. Guidry, D.A. Lamprecht, John H. Adamson, Vineel P.
1341 Reddy, Krishna C. Chinta, J.H. Mazorodze, Joel N. Glasgow, M. Richard-
1342 Greenblatt, A. Gomez-Velasco, H. Bach, Y. Av-Gay, H. Eoh, K. Rhee, and
1343 Adrie J.C. Steyn. 2016. Ergothioneine maintains redox and bioenergetic
1344 homeostasis essential for drug susceptibility and virulence of *Mycobacterium*
1345 *tuberculosis*. *Cell Rep.* 14:572-585.
1346 Sarathy, J., L. Blanc, N. Alvarez-Cabrera, P. O'Brien, I. Dias-Freedman, M. Mina, M.
1347 Zimmerman, F. Kaya, H.P. Ho Liang, B. Prideaux, J. Dietzold, P. Salgame, R.M.
1348 Savic, J. Linderman, D. Kirschner, E. Pienaar, and V. Dartois. 2019.
1349 Fluoroquinolone efficacy against tuberculosis is driven by penetration into lesions
1350 and activity against resident bacterial populations. *Antimicrob Agents Chemother*
1351 63:e02516-02518.
1352 Seaver, L.C., and J.A. Imlay. 2001. Hydrogen peroxide fluxes and compartmentalization
1353 inside growing *Escherichia coli*. *J. Bacteriol.* 183:7182-7189.
1354 Shandil, R.K., R. Jayaram, P. Kaur, S. Gaonkar, B.L. Suresh, B.N. Mahesh, R. Jayashree,
1355 V. Nandi, S. Bharath, and V. Balasubramanian. 2007. Moxifloxacin, ofloxacin,
1356 sparfloxacin, and ciprofloxacin against *Mycobacterium tuberculosis*: evaluation of
1357 *in vitro* and pharmacodynamic indices that best predict *in vivo* efficacy. *Antimicrob.*
1358 *Agents Chemother.* 51:576.
1359 Shapleigh, J.P. 2009. Dissimilatory and assimilatory nitrate reduction in the purple
1360 photosynthetic bacteria. In The purple phototrophic bacteria. Advances in
1361 photosynthesis and respiration. D.F. Hunter C.N., Thurnauer M.C., Beatty J.T.,
1362 editor Springer, Dordrecht, 623-642.

1363 Singh, A., D.K. Crossman, D. Mai, L. Guidry, M.I. Voskuil, M.B. Renfrow, and A.J.C.
1364 Steyn. 2009. *Mycobacterium tuberculosis* WhiB3 maintains redox homeostasis by
1365 regulating virulence lipid anabolism to modulate macrophage response. *PLoS*
1366 *Pathog.* 5:e1000545.
1367 Singh, A., D. Mai, A. Kumar, and A.J.C. Steyn. 2006. Dissecting virulence pathways of
1368 *Mycobacterium tuberculosis* through protein–protein association. *Proc. Natl. Acad.*
1369 *Sci. U.S.A.* 103:11346.
1370 Singh, S., N.P. Kalia, P. Joshi, A. Kumar, P.R. Sharma, A. Kumar, S.B. Bharate, and I.A.
1371 Khan. 2017. Boeravinone B, a novel dual inhibitor of NorA bacterial efflux pump of
1372 *Staphylococcus aureus* and human p-glycoprotein, reduces the biofilm formation
1373 and intracellular invasion of bacteria. *Front. Microbiol.* 8:1868.
1374 Sohaskey, C.D. 2008. Nitrate enhances the survival of *Mycobacterium tuberculosis*
1375 during inhibition of respiration. *J. Bacteriol.* 190:2981-2986.
1376 Sommer, I., H. Schwebel, V. Adamo, P. Bonnabry, L. Bouchoud, and F. Sadeghipour.
1377 2020. Stability of N-Acetylcysteine (NAC) in standardized pediatric parenteral
1378 nutrition and evaluation of N,N-Diacetylcystine (DAC) formation. *Nutrients* 12:
1379 Srinivas, V., M.L. Arrieta-Ortiz, A. Kaur, E.J.R. Peterson, and N.S. Baliga. 2020. PerSort
1380 facilitates characterization and elimination of persister subpopulation in
1381 mycobacteria. *m Systems* 5:e01127-01120.
1382 Steyn, A.J.C., J. Joseph, and B.R. Bloom. 2003. Interaction of the sensor module of
1383 *Mycobacterium tuberculosis* H37Rv KdpD with members of the Lpr family. *Mol.*
1384 *Microbiol.* 47:1075-1089.

1385 Tan, M.P., P. Sequeira, W.W. Lin, W.Y. Phong, P. Cliff, S.H. Ng, B.H. Lee, L. Camacho,
1386 D. Schnappinger, S. Ehrt, T. Dick, K. Pethe, and S. Alonso. 2010. Nitrate
1387 respiration protects hypoxic *Mycobacterium tuberculosis* against acid and reactive
1388 nitrogen species stresses. *PLoS One* 5:e13356.
1389 Taneja, N.K., and J.S. Tyagi. 2007. Resazurin reduction assays for screening of anti-
1390 tubercular compounds against dormant and actively growing *Mycobacterium*
1391 *tuberculosis*, *Mycobacterium bovis* BCG and *Mycobacterium smegmatis*. *J.*
1392 *Antimicrob. Chemother.* 60:288-293.
1393 Titov, D.V., V. Cracan, R.P. Goodman, J. Peng, Z. Grabarek, and V.K. Mootha. 2016.
1394 Complementation of mitochondrial electron transport chain by manipulation of the
1395 NAD+/NADH ratio. *Science* 352:231-235.
1396 Vilchèze, C., T. Hartman, B. Weinrick, and W.R. Jacobs. 2013. Mycobacterium
1397 tuberculosis is extraordinarily sensitive to killing by a vitamin C-induced Fenton
1398 reaction. *Nature Communications* 4:1881.
1399 Vilchèze, C., T. Hartman, B. Weinrick, P. Jain, T.R. Weisbrod, L.W. Leung, J.S.
1400 Freundlich, and W.R. Jacobs. 2017. Enhanced respiration prevents drug tolerance
1401 and drug resistance in *Mycobacterium tuberculosis*. *Proc. Natl. Acad. Sci. U.S.A.*
1402 114:4495-4500.
1403 Vilchèze, C., and W.R. Jacobs. 2021. The promises and limitations of N- acetylcysteine
1404 as a potentiator of first-line and second-line tuberculosis drugs. *Antimicrob. Agents*
1405 *Chemother.* AAC.01703-01720.
1406 Vilchèze, C., T.R. Weisbrod, B. Chen, L. Kremer, M.H. Hazbón, F. Wang, D. Alland, J.C.
1407 Sacchettini, and W.R. Jacobs, Jr. 2005. Altered NADH/NAD+ ratio mediates

1408 coresistance to isoniazid and ethionamide in mycobacteria. *Antimicrob. Agents*
1409 *Chemother.* 49:708-720.
1410 Vinogradov, A.D., and V.G. Grivennikova. 2016. Oxidation of NADH and ROS production
1411 by respiratory complex I. *Biophys. Acta Bioenerg.* 1857:863-871.
1412 Voskuil, M., I. Bartek, K. Visconti, and G. Schoolnik. 2011. The response of
1413 *Mycobacterium tuberculosis* to reactive oxygen and nitrogen species. *Front.*
1414 *Microbiol.* 2:1-12.
1415 Voskuil , M.I., D. Schnappinger , K.C. Visconti , M.I. Harrell , G.M. Dolganov , D.R.
1416 Sherman , and G. Schoolnik. 2003. Inhibition of respiration by nitric oxide induces
1417 a *Mycobacterium tuberculosis* dormancy program. *J. Exp. Med.* 198:705-713.
1418 Wayne, L.G., and L.G. Hayes. 1996. An *in vitro* model for sequential study of shiftdown
1419 of *Mycobacterium tuberculosis* through two stages of nonreplicating persistence.
1420 *Infect. Immun.* 64:2062-2069.
1421 Wayne, L.G., and L.G. Hayes. 1998. Nitrate reduction as a marker for hypoxic shiftdown
1422 of *Mycobacterium tuberculosis*. *Tuber Lung Dis.* 79:127-132.
1423 Wayne, L.G., and H.A. Sramek. 1994. Metronidazole is bactericidal to dormant cells of
1424 *Mycobacterium tuberculosis*. *Antimicrob. Agents Chemother.* 38:2054-2058.
1425 WHO. 2013. Global tuberculosis report 2013. World Health Organization, Geneva.
1426 WHO. 2019. Global tuberculosis report 2019. World Health Organization, Geneva.
1427 Zhao, X., J.Y. Wang, C. Xu, Y. Dong, J. Zhou, J. Domagala, and K. Drlica. 1998. Killing
1428 of *Staphylococcus aureus* by C-8-methoxy fluoroquinolones. *Antimicrob. Agents*
1429 *Chemother.* 42:956-958.

1430 Zhao, X., C. Xu, J. Domagala, and K. Drlica. 1997. DNA topoisomerase targets of the
1431 fluoroquinolones: a strategy for avoiding bacterial resistance. *Proc. Natl. Acad. Sci.*
1432 *U.S.A.* 94:13991-13996.

1433
1434
1435
1436
1437
1438
1439
1440
1441
1442
1443
1444
1445
1446
1447
1448
1449
1450
1451
1452

1453 **Figure legends**

1454 **Fig 1. Effect of moxifloxacin on biosensor oxidation, ROS level, and bacterial**
1455 **survival.** (**A**) Moxifloxacin increases oxidative stress that increases the ratio of oxidized
1456 (MSSM) to reduced mycothiol (MSH) via mycothiol-dependent peroxiredoxin (Prx) or
1457 peroxidase (Mpx). Oxidation of Mrx1-roGFP2 increases fluorescence intensity for
1458 excitation at ~400 nm and decreases it for excitation at ~490 nm. (**B**) Strain *M.*
1459 *tuberculosis*-roGFP2 was exposed to the indicated concentrations of moxifloxacin (1X
1460 MIC = 0.5 μM) for 48 h, and the ratiometric response of the biosensor and survival
1461 following treatment were determined. (**C**) Cells were treated as in panel B, and ROS were
1462 quantified by flow-cytometry using CellROX Deep Red dye. 10 mM cumene
1463 hydroperoxide (CHP) served as a positive control. Data represent mean fluorescence
1464 intensity of the dye. (**D**) Exponentially growing *M. tuberculosis* H37Rv was treated with
1465 moxifloxacin at the indicated concentrations for the indicated times; survival was
1466 assessed by determining colony-forming units (CFU). (**E**) Time-kill curves for *M.*
1467 *tuberculosis* treated with 10X MIC of moxifloxacin. Error bars represent standard
1468 deviation from the mean. Data represent at least two independent experiments performed
1469 in at least duplicate. Statistical significance is calculated against the no-treatment control
1470 (****$p < 0.0001$, *** $p < 0.001$, and **$p < 0.01$, *$p < 0.05$).

1471 **Fig 2. ROS mitigation reduces moxifloxacin-mediated killing of *M. tuberculosis*.** (**A**)
1472 Plan for detecting thiourea (TU) and bipyridyl (BP) effects on moxifloxacin lethality. (**B**)
1473 Exponentially growing *M. tuberculosis* H37Rv cultures were either left untreated or treated
1474 with 10 mM TU for 1 h before addition of the indicated concentrations of moxifloxacin
1475 (MOXI; 1X MIC = 0.5 μM) for 10 days followed by determination of CFU. (**C**) Effect of

1476 bipyridyl. *M. tuberculosis* as in *B* was untreated or treated with 250 μM BP for 15 min
1477 prior to addition moxifloxacin as in *B*. (**D**) The Mrx1-roGFP2 biosensor ratiometric
1478 response was determined after 48 h treatment of *M. tuberculosis* cultures with the
1479 indicated concentrations of MOXI alone or with 250 μM of BP. (**E**) *M. tuberculosis* cultures
1480 were treated with moxifloxacin, the drug was removed by washing, and cells were plated
1481 on drug-free 7H11 agar with or without catalase followed by CFU determination. (**F**) *M.*
1482 *tuberculosis* cultures were treated with 1X MIC of moxifloxacin for the indicated times,
1483 washed, and plated with or without catalase (17.5 U/mL of agar). Percentage survival was
1484 calculated relative to CFU of cultures at 0 h. Statistical significance was calculated
1485 between drug-alone group with drug + catalase group. Statistical considerations were as
1486 in Fig 1.

1487 **Fig 3. Whole-genome transcriptome profiling of *M. tuberculosis* treated with**
1488 **moxifloxacin.** (**A**) Heat-map showing expression changes due to 16-h treatment of *M.*
1489 *tuberculosis* with moxifloxacin. Differentially expressed genes (DEGs) exhibited a 2-fold
1490 change across all three treatment conditions (2X, 4X, and 8X MIC of moxifloxacin; 1X
1491 MIC = 0.4 μM); color code for the fold change is at the bottom of the second column
1492 (yellow: upregulated genes; turquois: down-regulated genes). Genes are grouped
1493 according to function. For genes belonging to bioenergetics processes, color code for the
1494 fold change is at the bottom of the fourth column. **sdhC* and *cmtR* are deregulated in two
1495 treatment conditions (2X and 4X) (**B**) Venn diagram showing transcriptome overlap
1496 between moxifloxacin-mediated (green circle) and H_2O_2-mediated stress for *M.*
1497 *tuberculosis* (Voskuil et al., 2011); DEGs obtained with treatment with 5 mM H_2O_2 for 40
1498 min and 5 mM H_2O_2 for 4 h are shown in beige and blue circles, respectively.

1499 **Fig 4. Moxifloxacin-mediated respiration arrest reversed by NAC.** (**A**) OCR
1500 (pmol/min) indicated oxygen consumption rate. Exponentially growing *M. tuberculosis*
1501 cultures were either left untreated (UT) or treated with 10X MIC of moxifloxacin (MOXI; 5
1502 μM) for the indicated times; black dotted lines indicate when MOXI or NAC (1 mM) or
1503 CCCP (10 μM) were added. Determination was via Seahorse XFp Analyzer (**B**) ECAR
1504 (mpH/min) indicated H^+ production or extracellular acidification due to glycolytic and TCA
1505 flux. Determination was as in OCR with data representing percentage of third baseline
1506 value. NAC (1 mM) addition enhanced OCR of (**C**) untreated and (**D***)* MOXI-treated cells.
1507 Data shown are representative of two independent experiments performed in triplicate.

1508 **Fig 5. Dissipation of NADH reductive stress diminishes moxifloxacin-induced ROS**
1509 **increase and lethality with *M. tuberculosis.*** Detection of **(A)** NADH or **(B)** NAD^+ levels.
1510 *M. tuberculosis* was treated with moxifloxacin (1X MIC = 0.5 μM), for 2 days, and NADH
1511 or NAD^+ levels were determined by an alcohol dehydrogenase-based redox cycling
1512 assay. **(C)** NADH/NAD^+ ratio. Untreated *M. tuberculosis* expressing *LbNox* served as a
1513 control. *p* was determined by unpaired two-tailed student's t-test analyzed relative to the
1514 untreated control. **(D)** ROS response to moxifloxacin. Wild-type *M. tuberculosis* H37Rv
1515 (WT *Mtb*) and cells expressing *Lbnox* (*LbNox*) were exposed to the indicated
1516 concentrations of moxifloxacin for 48 h, and ROS were quantified by flow-cytometry using
1517 CellROX Deep Red. **(E)** Cultures of exponentially growing wild-type *M. tuberculosis (*WT
1518 *Mtb)* and *LbNox* were treated with the indicated concentrations of moxifloxacin for 48 h,
1519 and survival was assessed by determining CFU. Statistical coniderations were as in Fig
1520 1 (**** $p < 0.0001$, *** and ### $p < 0.001$, ** $p < 0.01$, # $p < 0.05$, ns indicates not
1521 significant).

1522 **Fig 6. N-acetyl cysteine increases oxidative stress and moxifloxacin-mediated**
1523 **killing of *M. tuberculosis*.** NAC (1 mM) was administered 1 h before addition of
1524 moxifloxacin (MOXI; 1X MIC = 0.5 μM) at the indicated concentrations followed by 48 h
1525 incubation. **(A)** Experimental plan. (**B**) Oxidative stress, measured by the ratiometric
1526 response of the Mrx1-roGFP2 biosensor. (**C**) Bacterial survival, measured by plating on
1527 7H11 agar. **(D)** Effect of NAC and moxifloxacin combination with dormant bacilli. *M.*
1528 *tuberculosis* cultures were starved for nutrients for 14 days and then treated with
1529 moxifloxacin for 5 days in the presence or absence of NAC (1 mM) before determination
1530 of survival. Rifampicin (25 μM) served as a positive control. **(E)** NAC (1 mM) was added
1531 when cultures were placed in Vacutainer tubes followed by the treatment conditions
1532 indicated in Fig S2A and S2D. Metronidazole (Mtz; 10 mM) served as a positive control.
1533 Statistical considerations were as in Fig 1.

1534 **Fig 7. Moxifloxacin-induced oxidative shift in E_{MSH} and killing of *M. tuberculosis***
1535 **inside macrophages.** THP-1 macrophages, infected with *Mtb*-roGFP2 (MOI = 1:10),
1536 were treated with moxifloxacin (MOXI; 1X MIC = 0.5 μM) immediately after infection and
1537 incubated for the indicated times. (**A**) ~10,000 infected macrophages were analyzed by
1538 flow cytometry to quantify changes in the E_{MSH} of *M. tuberculosis* subpopulations. (**B**)
1539 Bacterial survival kinetics after MOXI treatment of THP-1 macrophages infected with *Mtb*-
1540 roGFP2 (CFU determination). (**C**) *Mtb*-roGFP2-infected THP-1 macrophages were
1541 treated with MOXI at the indicated concentrations in presence or absence of NAC (1 mM)
1542 immediately after infection and incubated for the indicated times; analysis was as in *A.*
1543 (**D**) THP1 macrophages, infected by *Mtb*-roGFP2, were treated with NAC (1 mM or 2
1544 mM), MOXI (10 μM), or the combination of NAC plus MOXI at those concentrations. After

1545 the indicated incubation times, the bacterial load in the macrophages was determined by
1546 plating on drug-free agar. *p* was determined by two-tailed student's t-test compared to
1547 MOXI-alone treatment at each time-point. Statistical considerations were as in Fig 1.

1548 **Fig 8. NAC decreases MDR *M. tuberculosis* survival in mice when combined with**
1549 **moxifloxacin. (A)** Experimental protocol. **(B** and **C)** Bacterial CFUs were enumerated
1550 from lungs and spleen at the indicated times. *p* was determined by unpaired two-tailed
1551 student's t-test analyzed relative to vehicle control treatment (** $p \leq 0.01$, *** $p \leq 0.001$;
1552 ns indicates not significant). Statistical significance between moxifloxacin (MOXI) alone
1553 and MOXI + NAC treatment is also shown (# $p < 0.05$, ## $p \leq 0.01$). Error bars represent
1554 standard deviation from the mean of bacterial burden in 5 mice per group.

1555 **Fig 9. Moxifloxacin-mediated killing of *M. tuberculosis* involves accumulation of**
1556 **NADH-dependent ROS, which is further enhanced by NAC.** (a) Moxifloxacin enters
1557 *M. tuberculosis* and traps gyrase on DNA as reversible, bacteriostatic drug-enzyme-DNA
1558 complexes in which the DNA is broken. The bacterium responds by down-regulating the
1559 expression of genes involved in respiration. The transcriptional changes result in reduced
1560 rate of respiration. NADH levels and the ratio of NADH to NAD^+ increase. NADH increases
1561 the free Fe^{2+} pool by releasing Fe from ferritin-bound forms and keeps it in a reduced
1562 state. ROS damage macromolecules in a self-amplifying process, as indicated by
1563 exogenous catalase blocking killing when added after removal of moxifloxacin. (b)
1564 Addition of N-acetyl cysteine to cells stimulates respiration and provides more ROS from
1565 moxifloxacin-mediated lesions. NAC alone does not induce ROS or trigger death. The
1566 additional ROS increases killing by moxifloxacin. Repair of moxifloxacin-mediated

1567 lesions, NADH dissipation, Fe sequestration, and ROS detoxification mechanisms
1568 contribute to survival.
1569

1570 **Figures**

1571

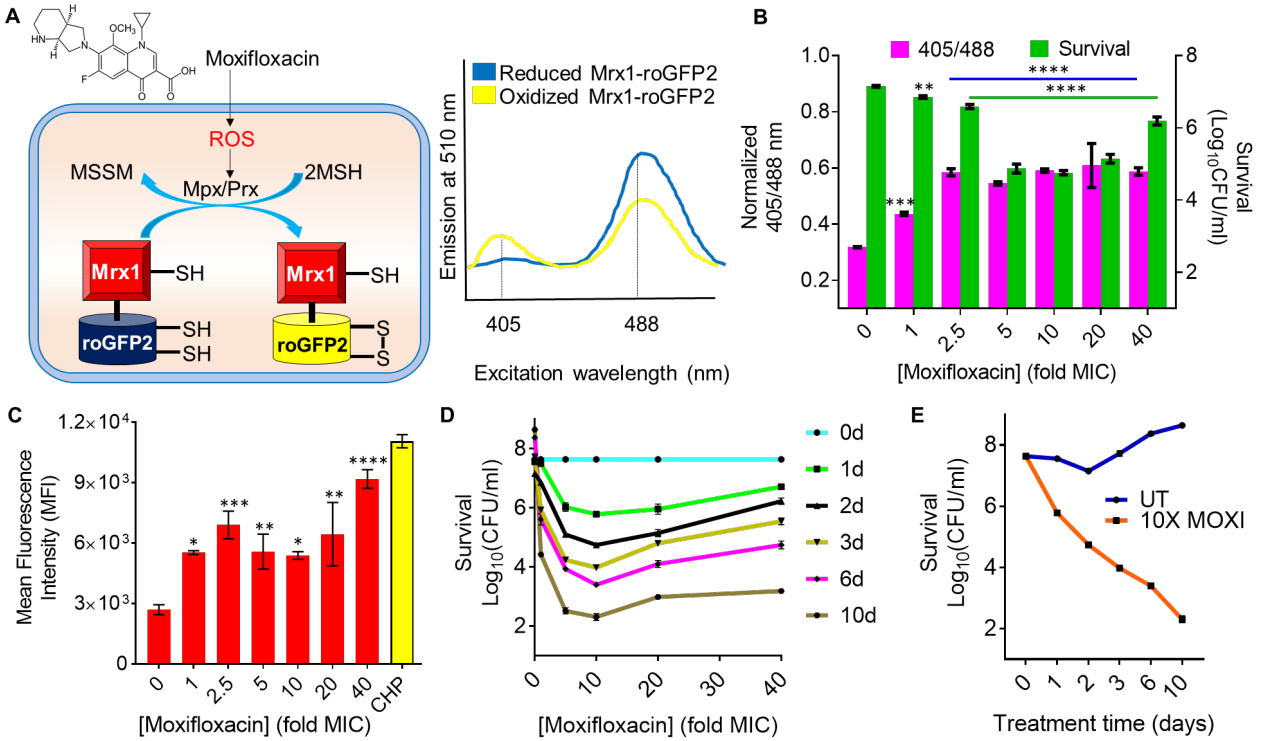

1572

1573 **Fig 1. Effect of moxifloxacin on biosensor oxidation, ROS level, and bacterial**

1574 **survival.**

1575

1576

1577

1578

1579

1580

1581

1582

1583

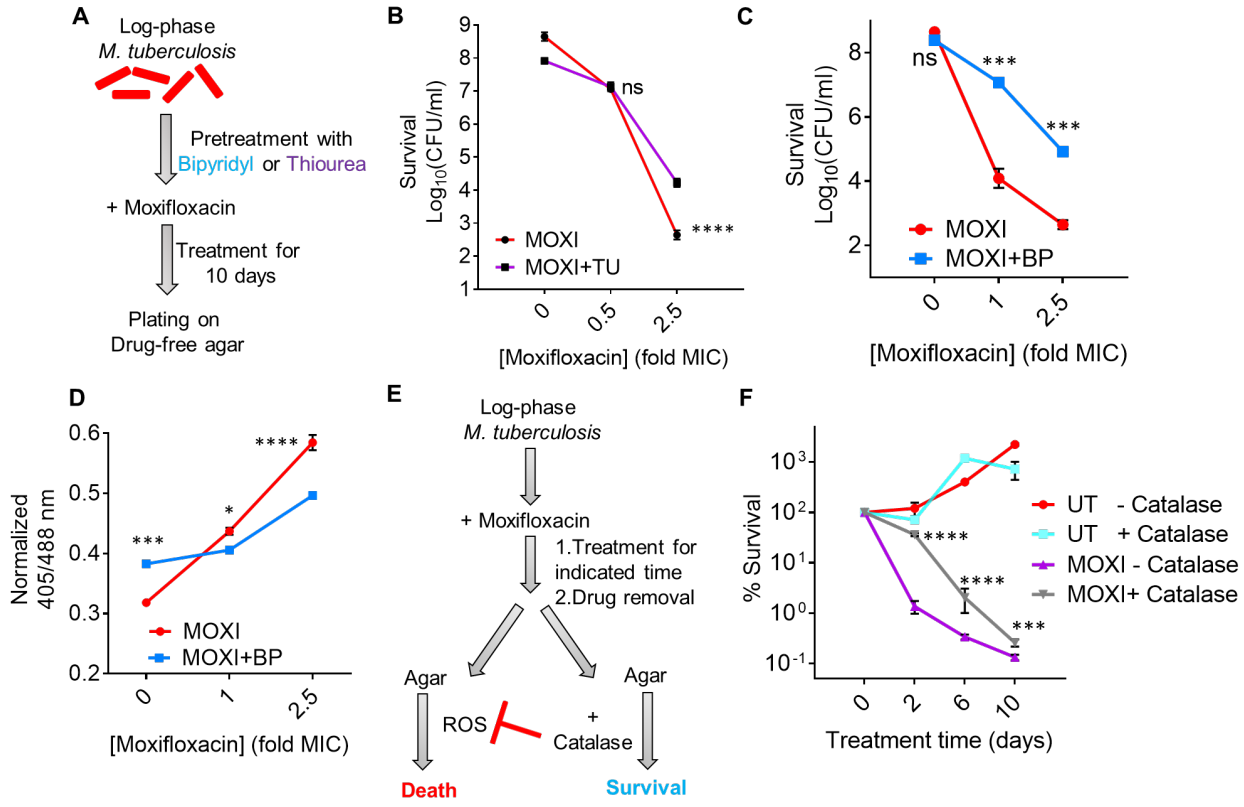

1584

1585 **Fig 2. ROS mitigation reduces moxifloxacin-mediated killing of *M. tuberculosis*.**

1586

1587

1588

1589

1590

1591

1592

1593

1594

1595

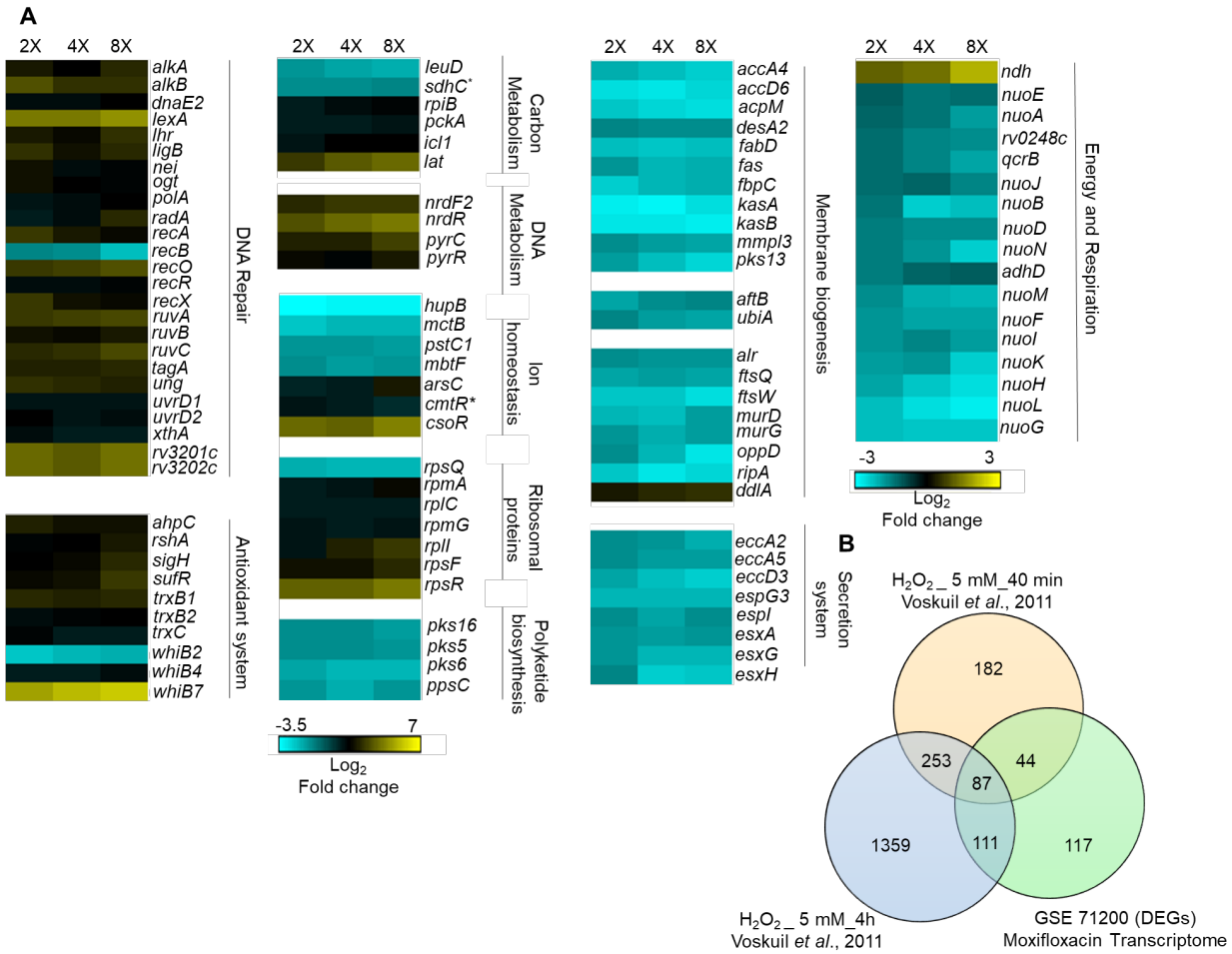

1596

1597 **Fig 3. Whole-genome transcriptomic profiling of *M. tuberculosis* treated with**

1598 **moxifloxacin.**

1599

1600

1601

1602

1603

1604

1605

1606

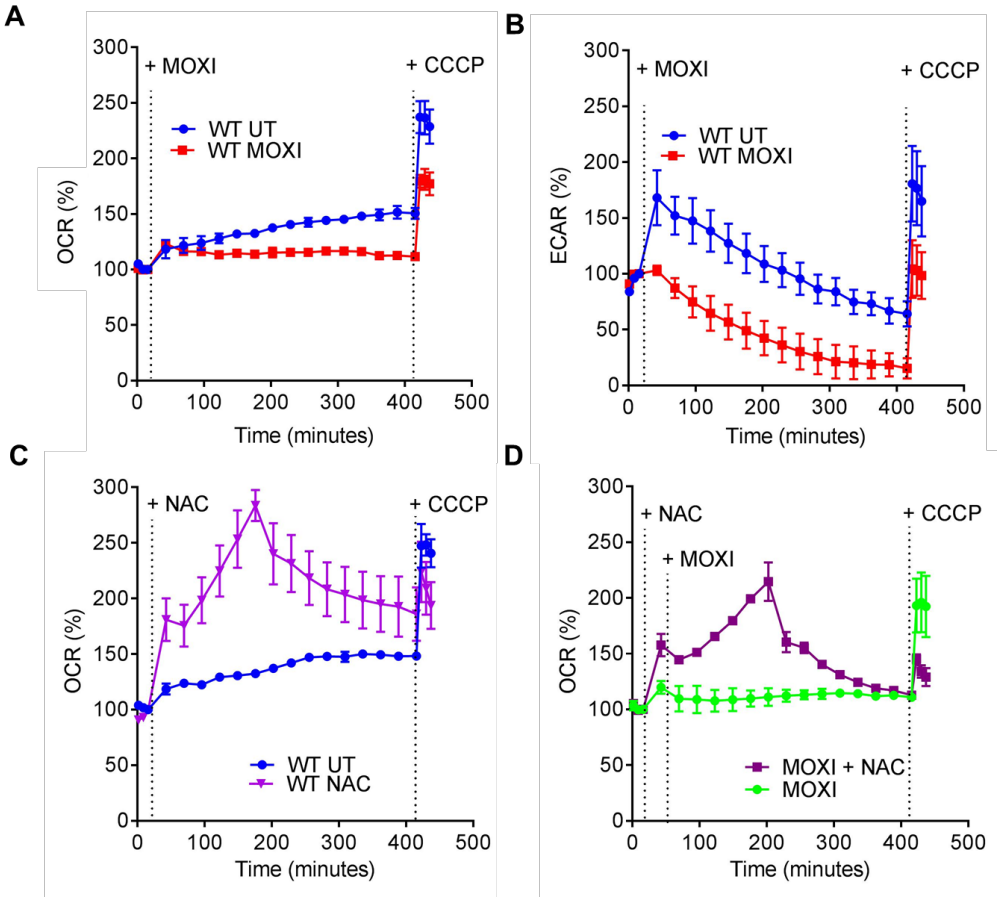

1607

1608 **Fig 4. Moxifloxacin-mediated respiration arrest reversed by NAC.**

1609

1610

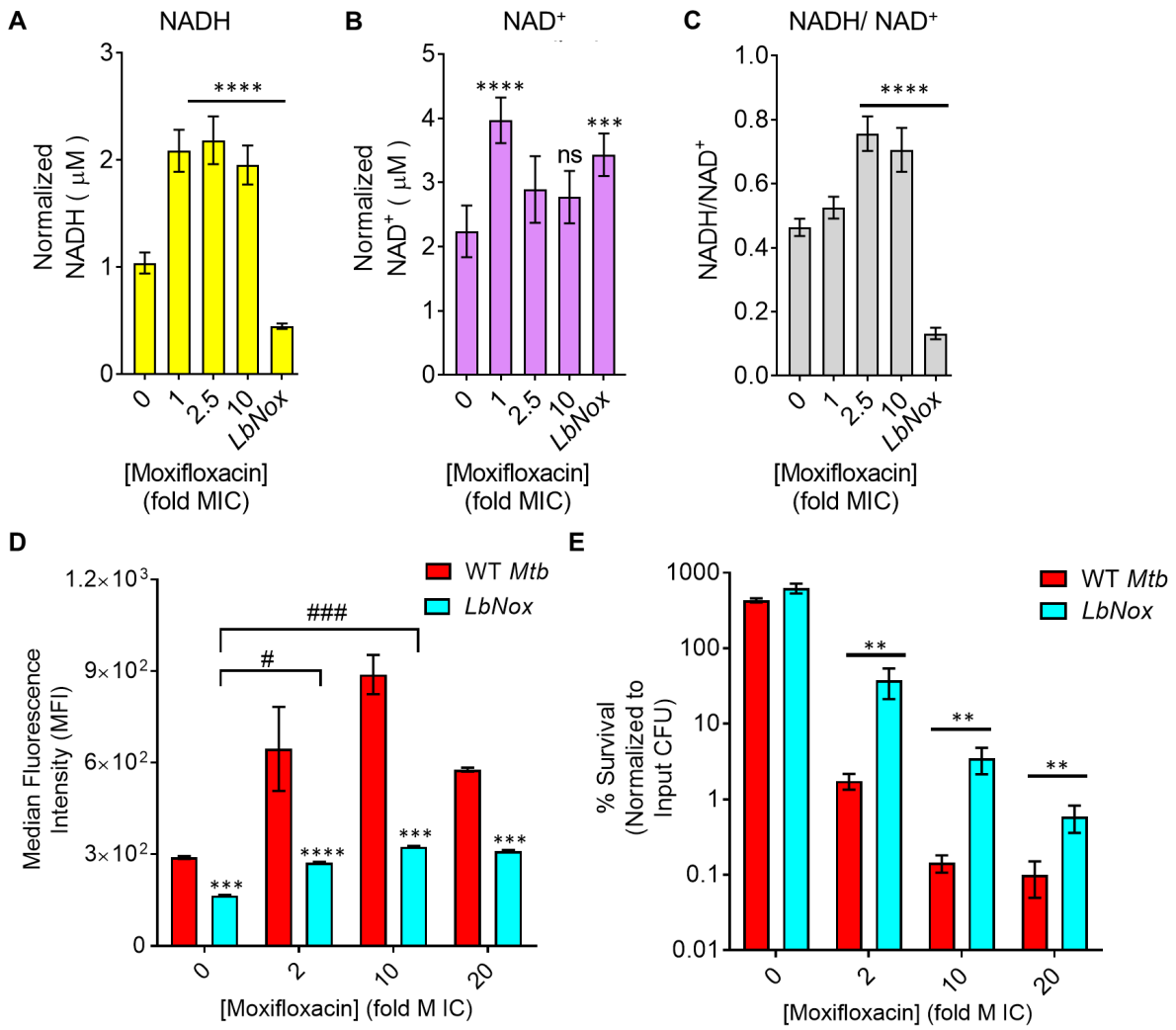

1611

1612 **Fig 5. Dissipation of NADH reductive stress diminishes moxifloxacin-induced**

1613 **ROS increase and lethality with *M. tuberculosis.***

1614

1615

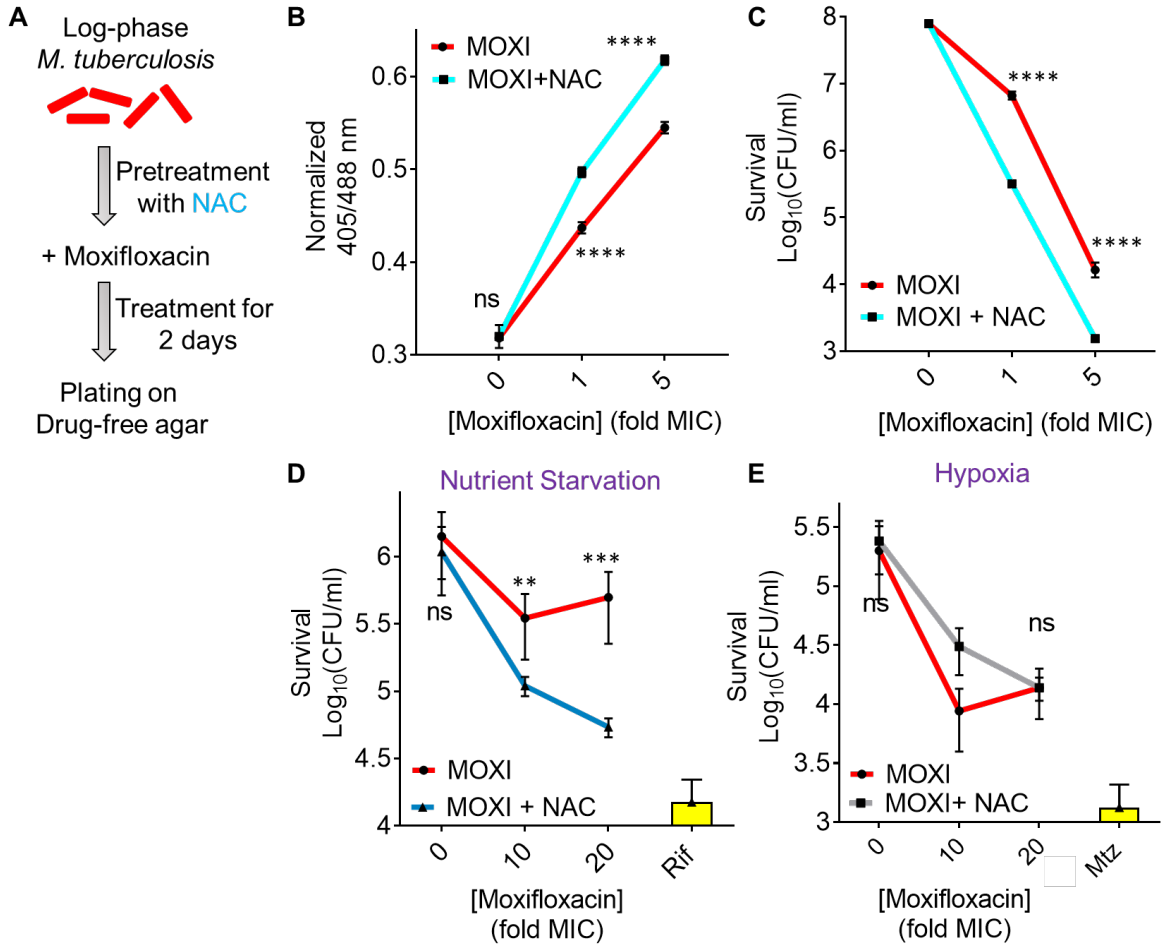

1616

1617 **Fig 6. N-acetyl cysteine increases oxidative stress and moxifloxacin-mediated**

1618 **killing of *M. tuberculosis*.**

1619

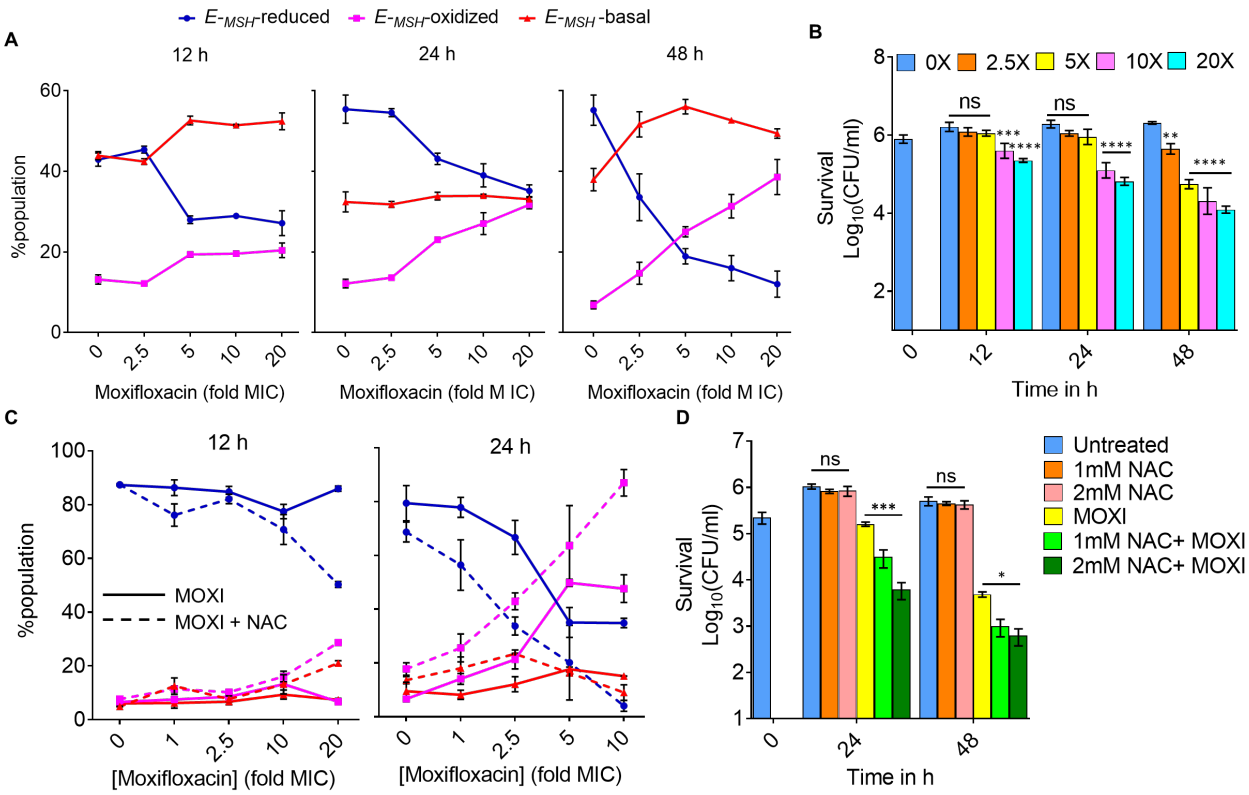

Fig 7. Moxifloxacin-induced oxidative shift in E_{MSH} and killing of *M. tuberculosis* inside macrophages.

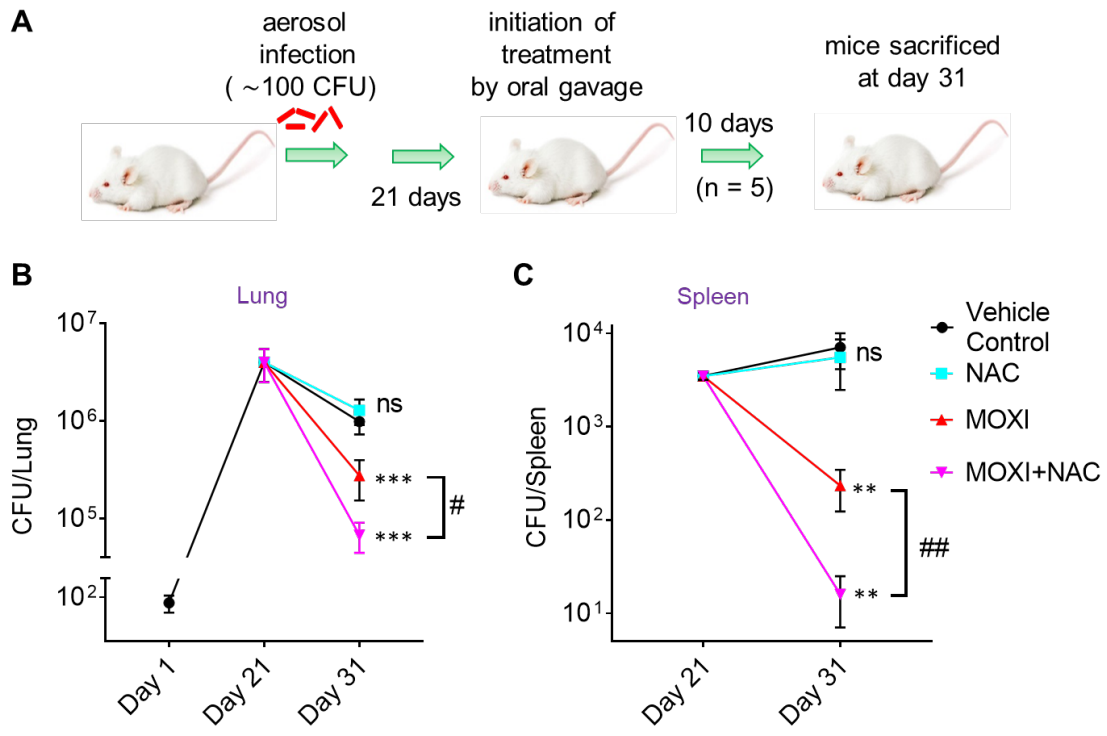

1625

1626 **Fig 8. NAC decreases MDR *M. tuberculosis* survival in mice when combined with**

1627 **moxifloxacin.**

1628

1629

1630

1631

1632

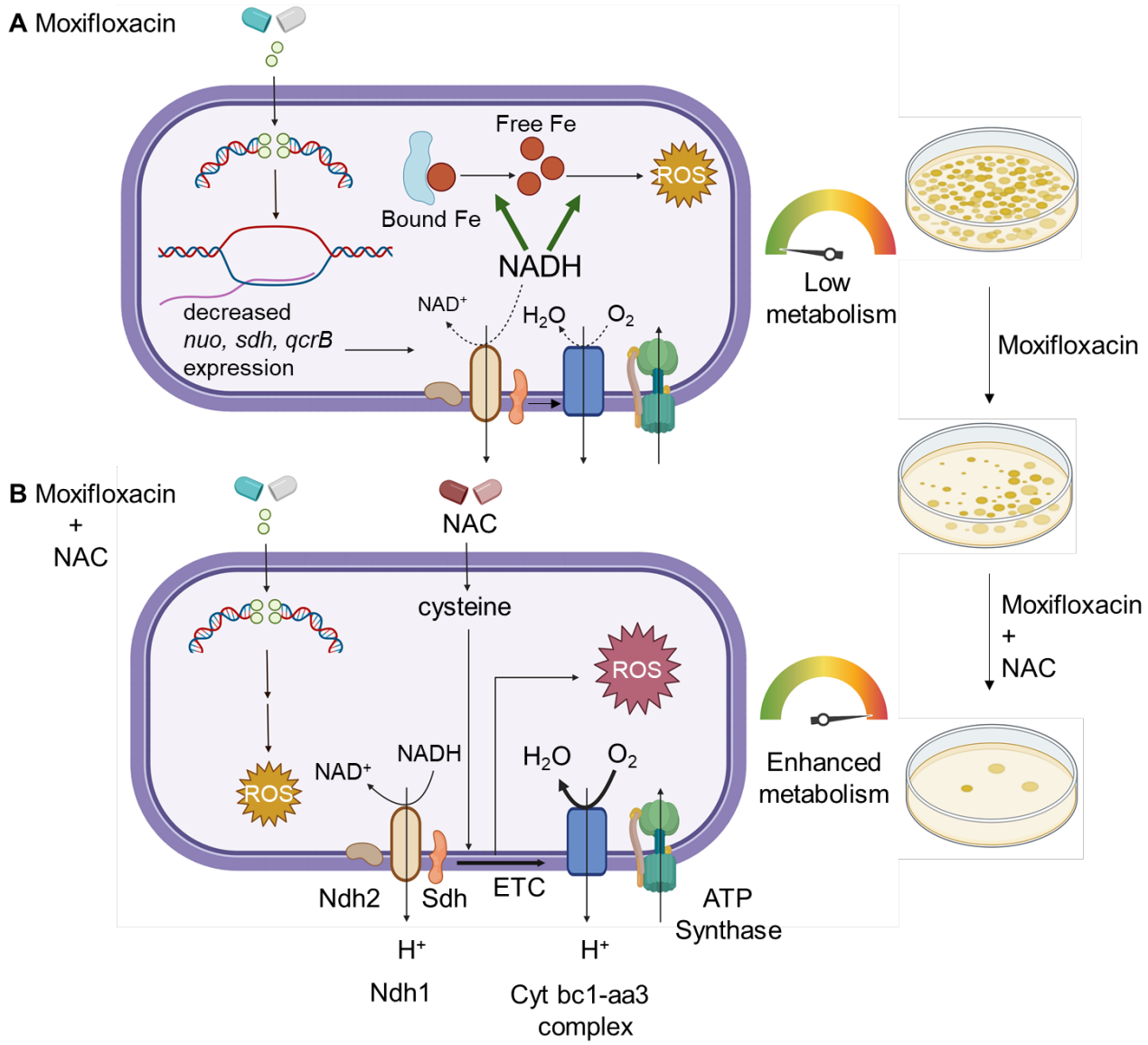

1633

1634 **Fig 9. Moxifloxacin-mediated killing of *M. tuberculosis* enhanced by NAC.**

1635